Neoarchaean to earliest Palaeoproterozoic magmatism in the southern Gawler Craton: petrogenesis of the Minbrie Gneiss and Carpa Granite

Claire E Wade and Stacey O McAvaney

Report Book
2016/00019

SOUTH AUSTRALIA
Government of South Australia
Department of State Development

Neoarchaean to earliest Palaeoproterozoic magmatism in the southern Gawler Craton: petrogenesis of the Minbrie Gneiss and Carpa Granite

Claire E Wade and Stacey O McAvaney

Geological Survey of South Australia,
Resources and Energy Group, DSD

January 2017

Report Book 2016/00019

Resources and Energy
Department of State Development
Level 7, 101 Grenfell Street, Adelaide
GPO Box 320, Adelaide SA 5001
Phone +61 8 8463 3037
Email dsd.minerals@sa.gov.au
www.minerals.statedevelopment.sa.gov.au

South Australian Resources Information Geoserver (SARIG)
SARIG provides up-to-date views of mineral, petroleum and geothermal tenements and other geoscientific data. You can search, view and download information relating to minerals and mining in South Australia including tenement details, mines and mineral deposits, geological and geophysical data, publications and reports (including company reports).
www.statedevelopment.sa.gov.au/sarig

Preferred way to cite this publication
Wade CE and McAvaney SO 2017. *Neoarchaean to earliest Palaeoproterozoic magmatism in the southern Gawler Craton: petrogenesis of the Minbrie Gneiss and Carpa Granite*, Report Book 2016/00019. Department for State Development, South Australia, Adelaide.

CONTENTS

TABLES

FIGURES

Neoarchaean to earliest Palaeoproterozoic magmatism in the southern Gawler Craton: petrogenesis of the Minbrie Gneiss and Carpa Granite

Claire E Wade and Stacey O McAvaney

ABSTRACT

This report presents geochemical constraints on the evolution of the Minbrie Gneiss and Carpa Granite, two magmatic units occurring in the southern Gawler Craton. These two units were previously assigned to the Palaeoproterozoic Lincoln Complex, however, recent geochronology has shown that they were emplaced over the interval c. 2520–2420 Ma and are therefore now recognised to be part of the Sleaford Complex (2570–2420 Ma).

The Minbrie Gneiss is a heterogeneous unit comprising a range of lithological types including granitic gneiss, quartz-feldspar-biotite migmatitic gneiss, and minor paragneiss and sills of amphibolite, and shows a range of magmatic crystallisation ages, from 2520–2420 Ma. The Minbrie Gneiss is magnesian, calc-alkalic to alkalic and peraluminous in composition and has a juvenile and very narrow range of $\varepsilon Nd_{(2520\ Ma)}$ values between -1.5 and 0 with a depleted mantle model age from 2.8–2.9 Ga. These isotopic compositions likely correspond to remelting of a source region similar in composition to the c. 2820 Ma Coolanie Gneiss, which crops out as a linear belt adjacent to the Minbrie Gneiss, and based on this observation is inferred to underlie it.

The Carpa Granite is a massive, unfoliated to weakly foliated, medium-grained, quartz-K-feldspar-plagioclase-biotite-muscovite±garnet granite to monzogranite. Magmatic crystallisation ages range from c. 2520 to c. 2515 Ma. The Carpa Granite is high silica, magnesian, alkali-calcic and peraluminous. $\varepsilon Nd_{(2520\ Ma)}$ values range from -6.4 to 2.8 and define distinct juvenile and evolved populations. Juvenile Carpa Granite has positive $\varepsilon Nd_{(2500\ Ma)}$ values (1.7 to 2.7), indicating a significant mantle component. Evolved Carpa Granite has negative $\varepsilon Nd_{(2500\ Ma)}$ values (-6.4 to -4.9), suggesting a significant crustal component, possibly reworking Mesoarchean (c. 2820 Ma Coolanie Gneiss or c. 3150 Ma Cooyerdoo Granite) basement.

INTRODUCTION

Early frameworks of the stratigraphy of the southern Gawler Craton recognised an Archean basement, termed the Sleaford Complex, which was intruded by a series of magmatic rocks known as the Lincoln Complex during a younger Palaeoproterozoic tectonothermal event, the Kimban Orogeny (Thomson, 1980, Parker *et al.*, 1985). Thus, deformed intrusive igneous rocks in the southern Gawler Craton were either mapped as part of the Archaean Sleaford Complex or Palaeoproterozoic Lincoln Complex, with the division into these two units assisted in part by Rb-Sr isotopic data (Webb *et al.*, 1986). The Lincoln Complex comprised a number of suites and intrusions spanning the time period c. 1850–1690 Ma, including the Donington Suite, Colbert Granite, Moody Suite, Wertigo Granite, Middlecamp Granite Carappee Granite, Minbrie Gneiss, Carpa Granite, Tournefort Dykes and Coolanie Gneiss (Parker, 1993).

However, subsequent U-Pb zircon geochronology redefined the time period of the Kimban Orogeny to 1730–1690 Ma (Hoek & Schaefer, 1998), and showed that the Lincoln Complex encompassed a number of units outside of this time period unrelated to the Kimban Orogeny, ranging from Mesoarchaean to Palaeoproterozoic (Fraser *et al.*, 2010, Fraser & Neumann, 2010, McAvaney *et al.*, 2016). Therefore, it is necessary to discontinue use of the term Lincoln Complex, and a new stratigraphic nomenclature is being developed for the rocks which were formerly part of the Lincoln Complex. These include the c. 3150 Ma Cooyerdoo Granite (Fraser *et al.*, 2010, McAvaney, 2012), the c. 2820 Ma Coolanie Gneiss (Fraser & Neumann, 2010), the c. 1850 Donington Suite (Hoek & Schaefer, 1998, Reid *et al.*, 2008a), the c. 1790–1770 Ma Wertigo Granite, c. 1775 Ma Tip Top Granite (McAvaney *et al.*, 2016), and the newly defined Peter Pan Supersuite (1745–1700 Ma), to encompass magmatism associated with the Kimban Orogeny (Wade & McAvaney, 2016, Wade *et al.*, 2016).

Two other former Lincoln Complex units, the Minbrie Gneiss and Carpa Granite, are now recognised to be part of the Sleaford Complex (2570–2420 Ma). The Sleaford Complex encompasses a range of lithologies from pelitic metasedimentary rocks, felsic to komatiitic volcanics and A- and S-type granites (Daly & Fanning, 1993, Teale *et al.*, 2000). The Sleaford Complex is lithologically similar to an equivalent-aged rock package in the northern Gawler Craton known as the Mulgathing Complex, and these two complexes are interpreted to have formed a contiguous package now separated by younger tectonism and cover sequences (Daly & Fanning, 1993, Reid *et al.*, 2014). Although some authors have interpreted the Sleaford Complex and Mulgathing Complex to have formed in a continental magmatic arc setting, these interpretations have relied heavily on data from the Mulgathing Complex (Swain *et al.*, 2005). Indeed, the lithological diversity, relatively poor exposure and lack of geochemical and isotopic data have meant that the tectonic setting and metallogenesis for the Sleaford Complex remains poorly understood. The purpose of this report is to present a summary of new geochemical and Sm-Nd isotopic data that has been acquired on the Minbrie Gneiss and Carpa Granite. The new data provides an insight into the petrogenesis of these two magmatic units and constraints on the geodynamic setting of for Sleaford Complex during the Neoarchaean to earliest Palaeoproterozoic.

GEOLOGICAL SETTING

The Gawler Craton, South Australia (Fig. 1), comprises a Mesoarchaean and Neoarchaean to earliest Palaeoproterozoic basement overlain and intruded by Palaeoproterozoic to Mesoproterozoic volcanosedimentary basins and igneous suites (Figs 1 & 2; Hand *et al.*, 2007, Reid & Hand, 2012).

The oldest exposed basement to the Gawler Craton is the c. 3150 Ma Cooyerdoo Granite, which is the product of melting of an older (c. 3400 Ma) tonalite-trondhjemite-granodiorite crust (Fraser *et al.*, 2010). The Cooyerdoo Granite is exposed only on northern Eyre Peninsula, but inherited zircons and Nd isotope values of younger igneous units indicate that it extends in the mid to lower crust to the central part of the Gawler Craton (Fraser *et al.*, 2010, McAvaney, 2012). The next event recorded in the Gawler Craton is the intrusion of the protolith of the c. 2820 Ma Coolanie Gneiss, an S-type granite which occurs on northeast Eyre Peninsula (Fraser & Neumann, 2010).

Overlying this older basement are deformed and metamorphosed rocks of the Sleaford and Mulgathing complexes, in the southern and northern Gawler Craton respectively (Fig. 1). The Mulgathing Complex forms the central-western portion of the Gawler Craton and includes the c. 2555 Ma Devil's Playground Volcanics, c. 2520 Ma Lake Harris Komatiite, metasedimentary rocks of the Christie Gneiss and interpreted felsic metavolcanics of the Kenella Gneiss (Daly and Fanning 1993). The Christie Gneiss contains a diverse lithological package including banded iron-formation, carbonates and extensive clastic sequences (Daly & Fanning, 1993, Swain *et al.*, 2005, Reid *et al.*, 2014). The Mulgathing Complex also includes a range of felsic and mafic intrusive rocks that were emplaced over the interval c. 2520–2480 Ma, and therefore during the time interval over which sedimentary rocks of the Christie Gneiss were being deposited (Reid *et al.*, 2014). The majority of the Mulgathing Complex underwent granulite facies metamorphism during the Sleafordian Orogeny (2475–2410 Ma) (McFarlane, 2006, Reid *et al.*, 2014, Halpin & Reid, 2016).

The Sleaford Complex occurs along the entire length of southern Gawler Craton (Fig. 1), and is best described from coastal exposures on the southern Eyre Peninsula. It comprises a sequence of volcanic, sedimentary and intrusive rocks spanning the interval 2520–2410 Ma, and includes the Hall Bay Volcanics, Wangary Gneiss, Carnot Gneiss and Dutton Suite, as well as the Minbrie Gneiss and Carpa Granite. The Sleaford Complex underwent metamorphism during the Sleafordian Orogeny, as well as during the Kimban Orogeny (1740–1690 Ma) (Daly & Fanning, 1993, Dutch *et al.*, 2008, Dutch *et al.*, 2010). The stratigraphy of the Sleaford Complex is described in more detail in the following section.

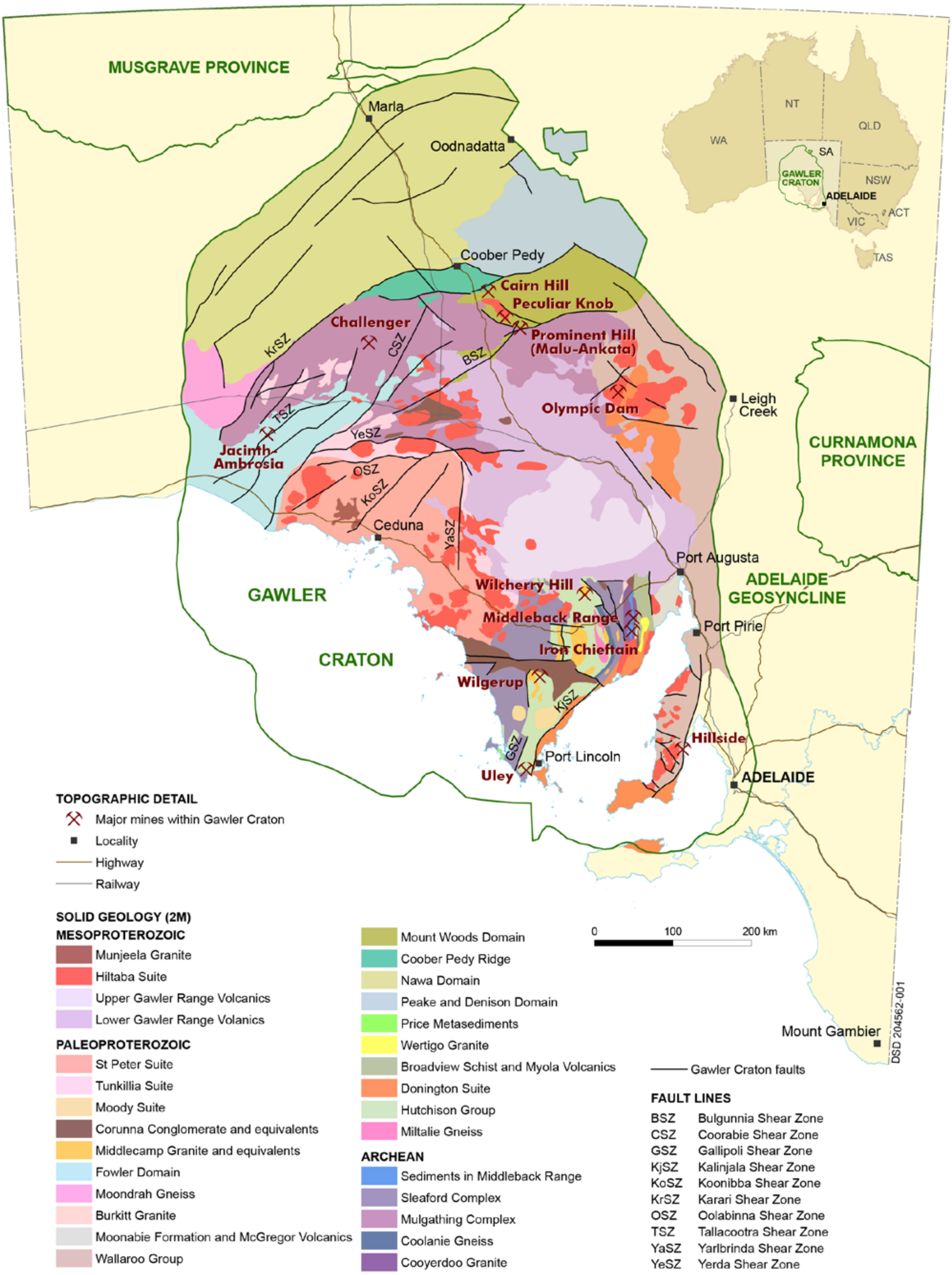

Figure 1. Interpreted solid geology of the Gawler Craton.

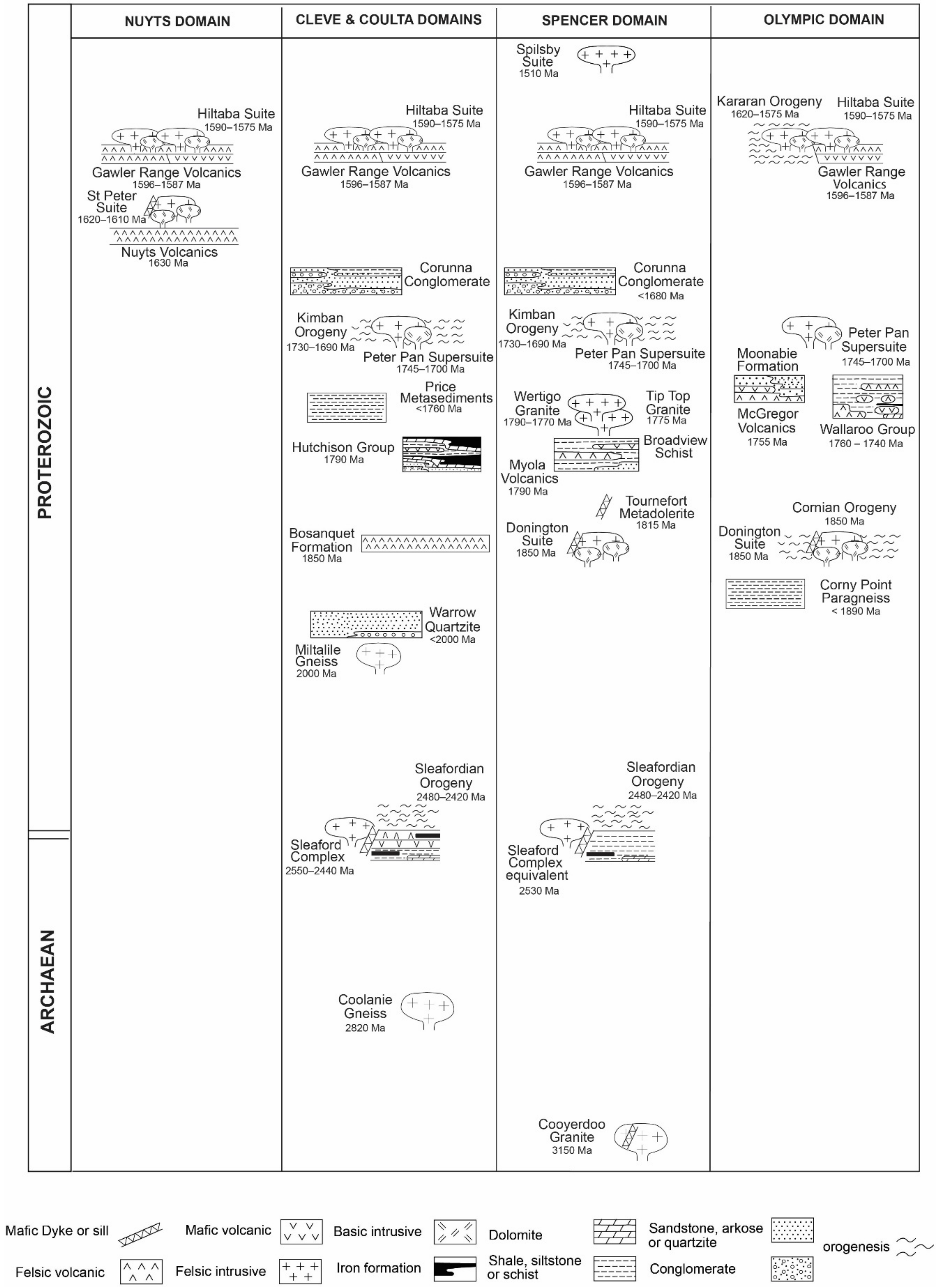

Figure 2. Time space plot for the southern Gawler Craton.

No geological activity was recorded in the Gawler Craton following the Sleafordian Orogeny until c. 2000 Ma, when the igneous precursor to the Miltalie Gneiss was emplaced (Fanning *et al.*, 2007). The intrusion of this granite heralds the beginning of prolonged basin formation and growth over the period c*.* 2000 to 1730 Ma, wherein large, lithologically complex shallow marine to continental basins were formed across the entire Gawler Craton (Cowley *et al.*, 2003, Payne *et al.*, 2006, Szpunar & Fraser, 2010, Szpunar *et al.*, 2011, Jagodzinski *et al.*, 2012, Lane *et al.*, 2015). Deposition during this phase of basin development was punctuated by the c. 1850 Ma Cornian Orogeny, comprising localised deformation and metamorphism and the emplacement of the Donington Suite along the eastern margin of the craton (Reid *et al.*, 2008a).

Sedimentation was terminated by the Kimban Orogeny (1740–1690 Ma), a major orogenic episode that affected the majority of the Gawler Craton (Parker, 1993, Dutch *et al.*, 2008). It resulted in greenschist to granulite facies metamorphism and high strain deformation largely partitioned into regional-scale transpressional belts, including the Kalinjala Mylonite Zone (Parker, 1980, Vassallo & Wilson, 2002). Widespread felsic and mafic magmatism also accompanied deformation of the Kimban Orogeny (Hand *et al.*, 2007). This magmatism includes the newly defined 1745–1700 Ma Peter Pan Supersuite (Wade and McAvaney, 2016). Post-orogenic granite intrusions are represented by the c.1690–1670 Ma Tunkillia Suite (Payne *et al.*, 2010).

The Kimban Orogeny and accompanying magmatism was synchronous with localised sedimentation in the Fowler Domain in the western Gawler Craton (c. 1740–1720 Ma; Howard *et al.*, 2011a) as well as clastic and bimodal volcanics of the Labyrinth Formation in the central Gawler Craton (c. 1715 Ma; Howard *et al.*, 2011b).

During the latest Palaeoproterozoic (i.e. 1680–1640 Ma) minor sedimentation is recorded in the Gawler Craton. This includes fluvial and alluvial sediments of the Corunna Conglomerate on Eyre Peninsula (c. 1680 Ma; McAvaney & Reid, 2008), and sandstone shale, dolomite and dacitic to andesitic volcanoclastic rocks of the Tarcoola Formation (c. 1655 Ma) in the central Gawler Craton (Daly, 1993). This was followed by a period of extended magmatism and volcanism from 1630–1570 Ma. In the southwestern part of the craton the felsic Nuyts Volcanics were extruded at c. 1630 Ma (Rankin *et al.*, 1990), and the felsic to mafic, juvenile St Peter Suite was intruded at 1647–1608 Ma (Swain *et al.*, 2008, Chalmers, 2009, Symington *et al.*, 2014, Reid *et al.*, 2016). This was followed by continued felsic volcanism in the central part of the craton, probably in a far-field continental back-arc setting, producing the c. 1595–1587 Ma Gawler Range Volcanics (Allen *et al.*, 2008, Jagodzinski *et al.*, 2016). The volcanics are comagmatic with high-T fractionated felsic and minor mafic intrusives of the c. 1595–1575 Ma Hiltaba Suite (Stewart & Foden, 2003).

Synchronous with extrusion of the Gawler Range Volcanics in the central part of the craton, deformation and metamorphism occurred in the northern and eastern parts of the craton during the c. 1600–1570 Ma Kararan Orogeny. This included amphibolite to granulite facies metamorphism in the Mount Woods Domain, Coober Pedy Ridge and Mabel Creek Ridge in the northern Gawler Craton (Hand *et al.*, 2007) and greenschist to lower amphibolite facies metamorphism on Yorke Peninsula in the eastern Gawler Craton. Deformation in the central Gawler Craton was partitioned into shear zones, including the east-west-trending Yerda Shear Zone and north-south-trending Yarlbrinda Shear Zone in the central Gawler Craton (Stewart, 2010), and the north-south-trending Bulgunnia Shear Zone along the southern margin of the Mount Woods Domain (Fraser & Lyons, 2006).

At c. 1560 Ma granulite facies metamorphism is recorded in the Nundroo block of the Fowler Domain and may be linked with the reactivation of the shear zones (Fanning *et al.*, 2007, Jagodzinski & Reid, 2016). Minor localised magmatism also occurred at this time in the Peake and Denison inliers in the northern Gawler Craton (1555–1530 Ma)(Fanning *et al.*, 2007). The youngest event recorded in the Gawler Craton consists of the reactivation of shear zones between c*.* 1470 and 1450 Ma at greenschist to amphibolite facies in the western Gawler Craton (Fraser & Lyons, 2006).

STRATIGRAPHY OF THE SLEAFORD COMPLEX

The term Sleaford Complex was first introduced by Thomson (1980) to describe late Archaean to early Palaeoproterozoic granites, orthogneisses and paragneisses on Eyre Peninsula. The Sleaford Complex occurs along the entire length of western Eyre Peninsula (Fig. 3), and is best described from coastal exposures on the southern Eyre Peninsula. It contains a number of formations, including the Hall Bay Volcanics, Wangary Gneiss, Carnot Gneiss and Dutton Suite (Swain *et al.*, 2005), as well as the Minbrie Gneiss and Carpa Granite, which are herein redefined to sit within the Sleaford Complex (Appendix 1).

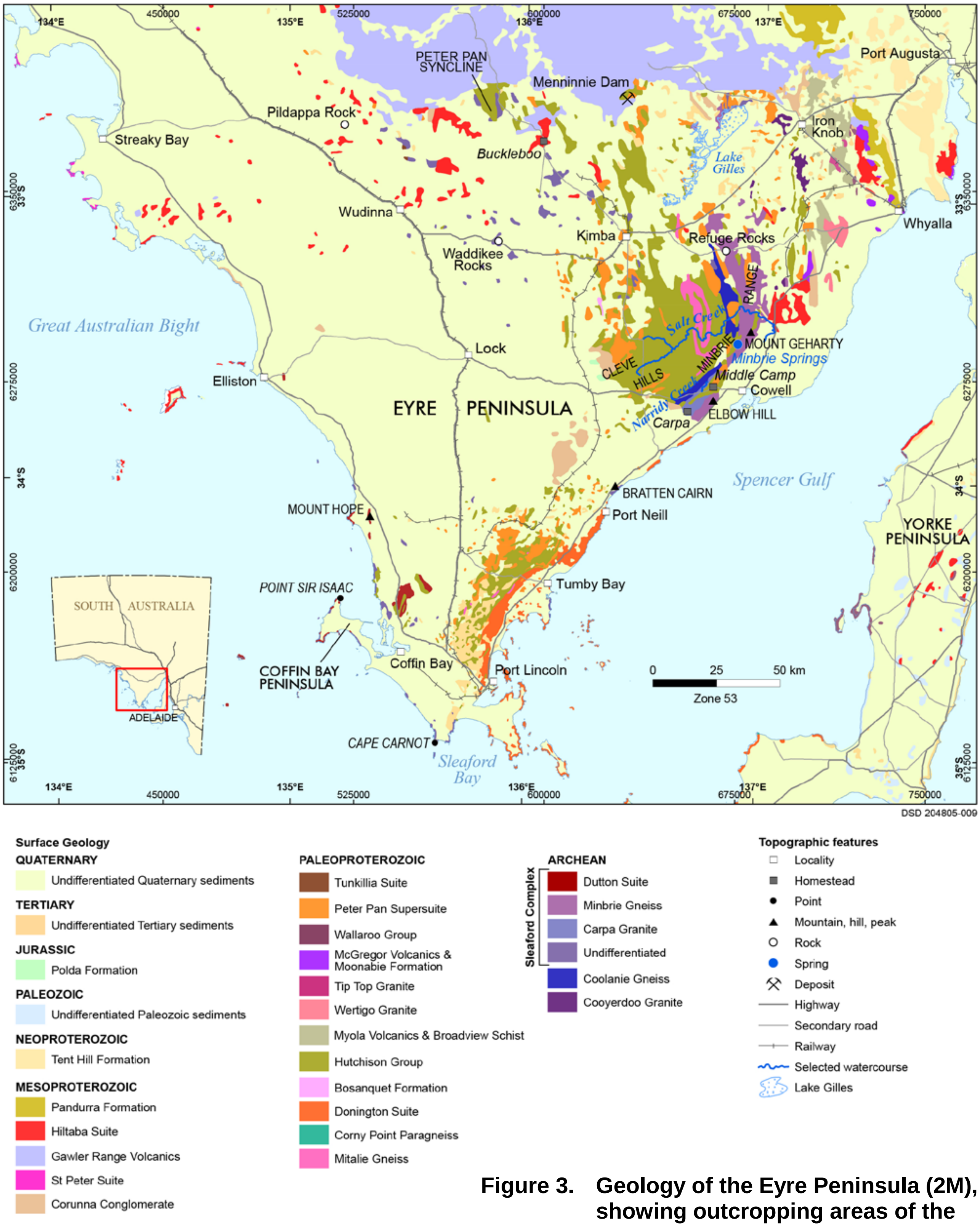

Figure 3. Geology of the Eyre Peninsula (2M), showing outcropping areas of the Sleaford Complex.

The Sleaford Complex comprises two phases: an older phase consisting of sedimentary units, felsic and mafic volcanics and igneous intrusives with maximum depositional ages and crystallization ages in the range 2600–2470 Ma, and a younger phase of intrusives emplaced during the Sleafordian Orogeny (2470–2410 Ma) (Table 1 and Fig. 4). The phases of sedimentation, magmatism and metamorphism in the Sleaford Complex are broadly similar to those recorded for the Mulgathing Complex.

Table 1. Summary of age ranges for metamorphism, magmatism and sedimentation in the Sleaford and Mulgathing Complexes. See Figure 4 for data sources.

	Sleaford Complex	Mulgathing Complex
Metamorphism	2510 ± 24 Ma – 2427 ± 4 Ma	2471 ± 5 Ma – 2409 ± 7 Ma
Magmatism	2529 ± 4 Ma – 2348 ± 21 Ma	2568 ± 6 Ma – 2428 ± 14 Ma
Sedimentation	2597 ± 8 Ma – ~ 2470 Ma	2550 ± 10 Ma – 2480 ± 4 Ma

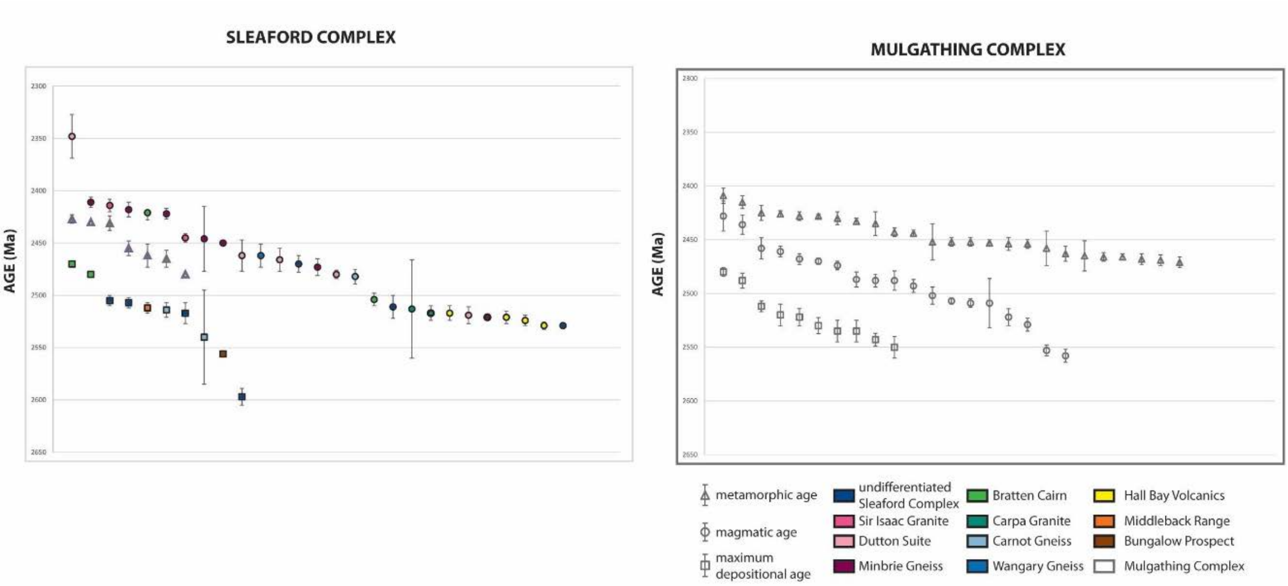

Figure 4. Metamorphic, magmatic and maximum depositional ages (with error bars) for the Sleaford and Mulgathing complexes. Data from Cowley & Fanning (1991), Dutch *et al.* (2010), Fanning *et al.* (2007), Fraser & Neumann (2010), Fraser *et al.* (2012), Jagodzinski & McAvaney (2016), Jagodzinski *et al.* (2006), Jagodzinski *et al.* (2007), Jagodzinski *et al.* (2009), Jagodzinski *et al.* (2012), Lane *et al.* (2011), McFarlane *et al.* (2007), Nebel *et al.* (2007), Reid (2007), Reid *et al.* (2014), Reid & Jagodzinski (2011), Swain *et al.* (2005), Teasdale (1997). Age calculations include Pb-Pb Kober zircon, U-Pb ID-TIMS zircon, U-Pb SHRIMP zircon, U-Pb LA-ICPMS zircon, U-Pb SHRIMP monazite, U-Pb LA-ICPMS monazite and U-Pb EPMA monazite.

HALL BAY VOLCANICS

The Hall Bay Volcanics are known only from drillholes near Mount Hope on western Eyre Peninsula (Fig. 3), and comprise a sequence of felsic volcanics and volcaniclastics interlayered with aluminous metapelites and evaporitic and iron-rich sediments. They are the oldest unit in the Sleaford Complex, with a magmatic age of 2520 ± 7 Ma (Teale *et al.*, 2000). The felsic volcanics are composed of corroded and embayed quartz phenocrysts and K-feldspar phenocrysts in a fine-grained groundmass (Fig. 5a; Teale *et al.*, 2000). The metasediments include metasandstone, andalusite-, kyanite-, garnet- and staurolite-bearing quartz-muscovite schist, carbonaceous phyllite, tremolite marble, and magnetite-rich pelite containing minor interbeds of calc-silicate, amphibolite and banded iron-formation (Teale *et al.*, 2000). The Hall Bay Volcanics are intruded by the Kiana Granite and Coulta Granodiorite of the Dutton Suite (see below), and were deformed to greenschist facies during the Kimban Orogeny (Teale *et al.*, 2000).

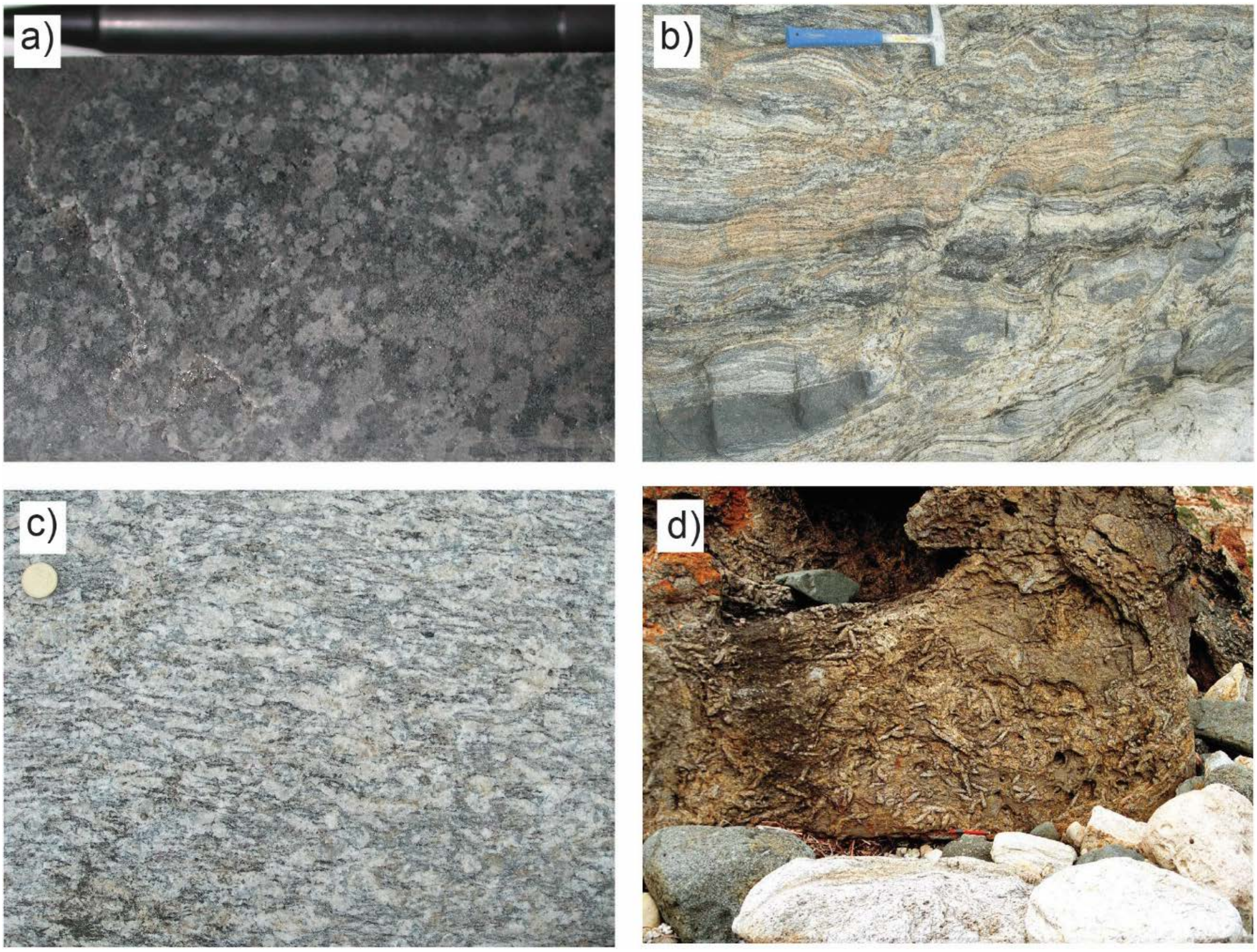

Figure 5. Units of the Sleaford Complex on southern Eyre Peninsula. (a) Calc-silicate altered felsic volcanic, Hall Bay Volcanics, in drillhole LINC 46 (photo 47998). **(b)** Carnot Gneiss interlayered with possible metasediment and mafic sills (photo courtesy of A. Reid). **(c)** Carnot Gneiss composed of K-feldspar augen in a gneissic matrix of K-feldspar-quartz-plagioclase-biotite-garnet (photo courtesy of A. Reid). **(d)** Wangary Gneiss containing pseudomorphs of andalusite (photo 48532).

CARNOT GNEISS

The Carnot Gneiss is a composite geological unit comprising felsic orthogneiss, metabasalt and siliciclastic paragneiss (Fig. 5b) exposed in coastal sections between Sleaford Bay and Cape Carnot on southern Eyre Peninsula (Fig. 3; Daly & Fanning, 1993). Paragneiss has maximum depositional ages of 2540 ± 45 Ma to 2514 ± 7 Ma (Lane, 2011, Jagodzinski *et al.*, 2012) and orthogneiss and granite has magmatic ages ranging from 2465 ± 8 Ma to 2431 ± 7 Ma (Dutch *et al.*, 2010, Jagodzinski *et al.*, 2012).

Paragneiss is composed of K-feldspar, plagioclase, quartz, garnet, biotite ± sillimanite ± cordierite (Daly & Fanning, 1993). Fine-grained mafic granulite bands 1–2 m thick within the paragneiss are composed of hypersthene, diopside and plagioclase, and are tholeiitic in composition and are interpreted to be either volcanic flows or intrusive sills (Daly & Fanning, 1993). Orthogneiss occurs concordant to the layering in the paragneiss and includes augen gneiss composed of K-feldspar augen in a gneissic matrix of K-feldspar-quartz-plagioclase-biotite-garnet, and granitic gneiss composed of plagioclase-hypersthene-diopside-K-feldspar-quartz-biotite (Fig. 5c; Daly & Fanning, 1993). The Carnot Gneiss was subject to granulite facies metamorphism during the Sleafordian Orogeny (2470–2420 Ma; Bradley, 1972, Fanning *et al.*, 1981, Daly *et al.*, 1998) and reworking during the Kimban Orogeny (1740–1690 Ma).

WANGARY GNEISS

The Wangary Gneiss is exposed southwest of Point Sir Isaac on Coffin Bay Peninsula (Fig. 3) and comprises a massive to layered K-feldspar-plagioclase-quartz-biotite-muscovite-andalusite gneiss (Fig. 5d). It is interpreted to have a metasedimentary and intermediate to felsic igneous protolith equivalent in age and composition to the Carnot Gneiss (Schwarz, 2003). The Wangary Gneiss underwent amphibolite facies metamorphism during the Sleafordian Orogeny, and is intruded by the Kiana Granite of the Dutton Suite (Schwarz, 2003). Reworking during the Kimban Orogeny, including high grade metamorphism and mylonite development (Dutch *et al.*, 2008), is also evident in the Wangary Gneiss.

DUTTON SUITE

The Dutton Suite (Parker *et al.*, 1985) comprises undeformed to foliated felsic plutonic rocks of the Sleaford Complex occurring on southern Eyre Peninsula (Fig. 3), and includes the Coulta Granodiorite, Kiana Granite and Whidbey Granite (Daly & Fanning, 1993). The Coulta Granodiorite intruded at c. 2520 Ma (Fanning *et al.*, 2007), the Kiana Granite at c. 2480 Ma (Jagodzinski *et al.*, 2012) and the Whidbey Granite at c. 2440 Ma (Webb *et al.*, 1986). The Coulta Granodiorite is a medium- to coarse-grained, foliated, grey granodiorite containing mafic xenoliths (Fig. 6a; Daly & Fanning, 1993). The Kiana Granite is a grey, K-feldspar-plagioclase-quartz-muscovite-biotite granite characterised by abundant, tabular K-feldspar and microcline phenocrysts up to 50 mm in size (Figs 6a and b; Daly & Fanning, 1993), and contains xenoliths of the Coulta Granodiorite (Daly & Fanning, 1993). The Whidbey Granite is composed of K-feldspar, microcline, quartz, plagioclase and minor biotite and contains partly digested mafic xenoliths (Fig. 6c and d; Daly & Fanning, 1993).

The Sir Isaac Granite, which crops out on the northern coast of Coffin Bay Peninsula, is interpreted to be equivalent to the Dutton Suite, with a magmatic crystallisation age of 2445 ± 4 Ma (Jagodzinski *et al.*, 2006). It is a garnet- and cordierite-bearing K-feldspar-quartz-plagioclase-biotite granite which contains a weak magmatic foliation defined by aligned tabular K-feldspar phenocrysts and euhedral to subhedral cordierite porphyroblasts up to 3 cm in length (Dutch, 2009).

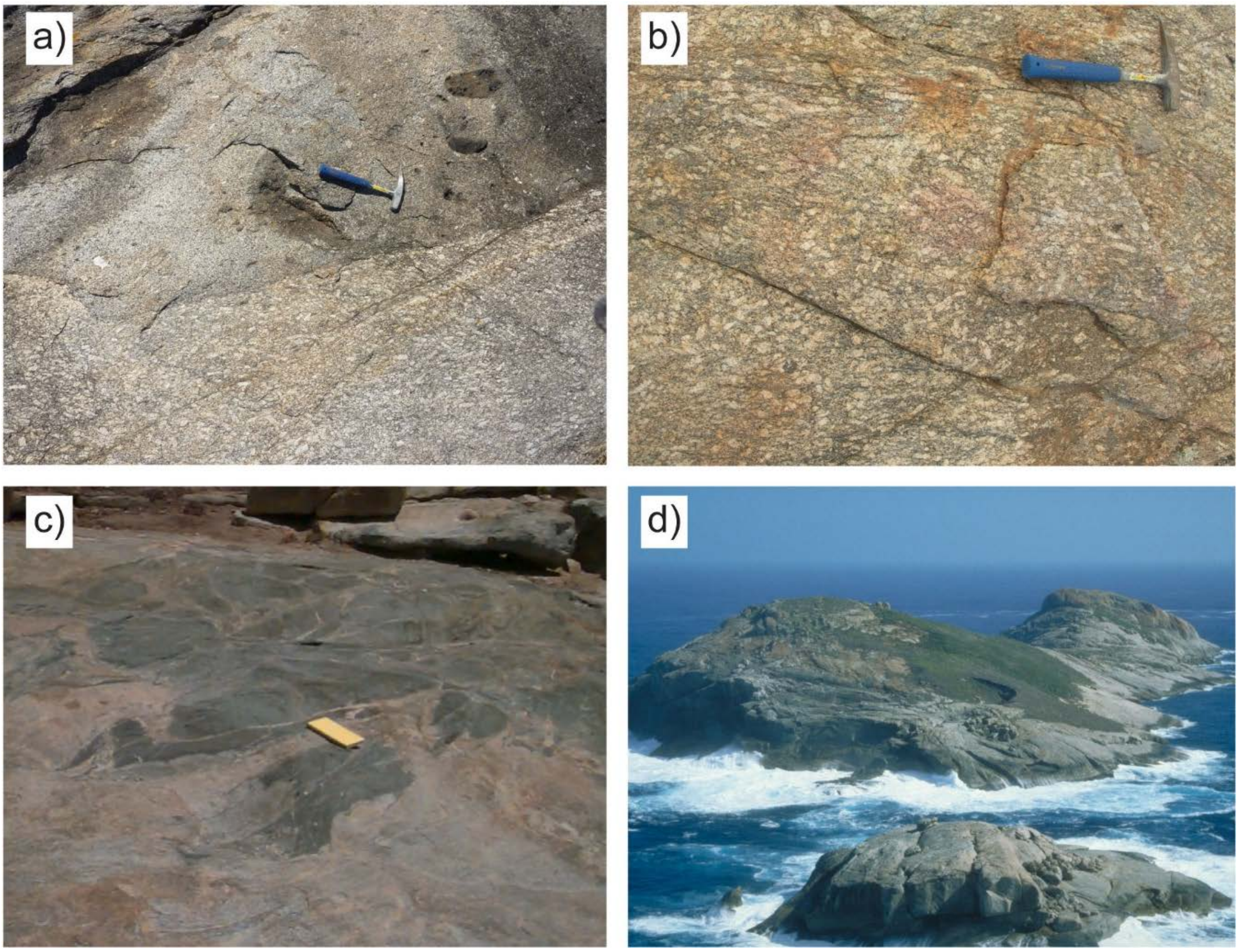

Figure 6. The Dutton Suite, Sleaford Complex. (a) Contact between grey Coulta Granodiorite, containing partly assimilated mafic xenoliths, and Kiana Granite with abundant tabular, K-feldspar phenocrysts, Mount Hope (photo courtesy of A. Reid). **(b)** Kiana Granite at Polda Rock (photo courtesy of A. Reid). **(c)** Whidbey Granite containing partly digested mafic xenoliths, Four Hummocks (photo 048536). **(d)** The Four Hummocks islands, composed predominantly of Whidbey Granite, 77 km southwest of Port Lincoln (photo 045934).

UNDIFFERENTIATED SLEAFORD COMPLEX ON NORTHERN EYRE PENINSULA

No stratigraphic nomenclature exists for exposures of the Sleaford Complex on central and northern Eyre Peninsula, where it is dominated by granitic gneiss and migmatitic orthogneiss, with lesser paragneiss, banded iron-formation and mafic granulite (Flint & Rankin, 1991, Parker & Fanning, 1998). In this area the Sleaford Complex is overlain by the Hutchison Group and is intruded by the 1745–1700 Ma Peter Pan Supersuite (Wade & McAvaney, 2016). It includes notable exposures west of Buckleboo Homestead, around the salt lakes northeast of Pondanna Rock, Waddikee Rocks, around the margins of the Peter Pan Dam syncline, basement in the Menninnie Dam area and along the northern shore of Lake Gilles (Fig. 3). As on the southern Eyre Peninsula, the protoliths to the Sleaford Complex on the northern Eyre Peninsula underwent metamorphism during the Sleafordian Orogeny, overprinted by deformation during the Kimban Orogeny.

West of Buckleboo Homestead the Sleaford Complex comprises grey garnet-quartz-feldspar-biotite ± cordierite gneiss, with garnets typically occurring in migmatitic and pegmatitic segregations, deformed by narrow shear bands (Parker & Fanning, 1998). Exposures of the Sleaford Complex along the margins of the salt lakes northeast of Pondanna Rock comprise megacrystic granitic gneiss composed of eudhedral to subhedral K-feldspar phenocrysts 1–3 cm in diameter, wrapped by a medium-grained quartz-K-feldspar-plagioclase-biotite gneissic fabric (Fig. 7a). At Waddikee Rocks the Sleaford Complex is a quartz-feldspar-biotite-garnet migmatite (Fig. 7b), which has a zircon age spectra consistent with either an meta-igneous precursor with inheritance or sedimentary precursor (Fraser & Neumann, 2010). The hinges of a regional syncline (Peter Pan Syncline), west of Peter Pan Dam, expose metagranite to granitic gneiss of the Sleaford Complex, composed of aligned tabular feldspar crystals up to ~2 cm in length, in a foliated medium-grained quartz-feldspar-biotite matrix (Fig. 7c). The granitic gneiss has an igneous crystallisation age of 2470 ± 8 Ma, recording high grade metamorphism at c. 2430 Ma and 1723 ± 13 Ma, and is intruded by gneissic granite of the Peter Pan Supersuite (Fig. 7d) (Fraser & Neumann, 2010). Sleaford Complex at Menninnie Dam comprises biotite-rich quartzofeldspathic gneiss with layering defined by quartzofeldspathic leucosomes, and has an igneous crystallisation age of 2511 ± 4 Ma (Fraser & Neumann, 2010).

Equivalents to the Sleaford Complex also occur along the northern shore of Lake Gilles (Fig. 3). They consist of an interlayered sequence of leucogranite and amphibolite intruding a metasedimentary package containing quartzofeldspathic paragneiss, mica schist and calc-silicate (Fig. 7e; Reid *et al.*, 2008b). A quartz-K-feldspar leucogneiss containing a shear fabric defined by quartz ribbons (Fig. 7f) yielded a zircon igneous crystallisation age of 2529 ± 4 Ma (Fraser & Neumann, 2010). The sequence is tightly to isoclinally folded about sub-horizontal north-northwest trending fold axes (Reid *et al.*, 2008b).

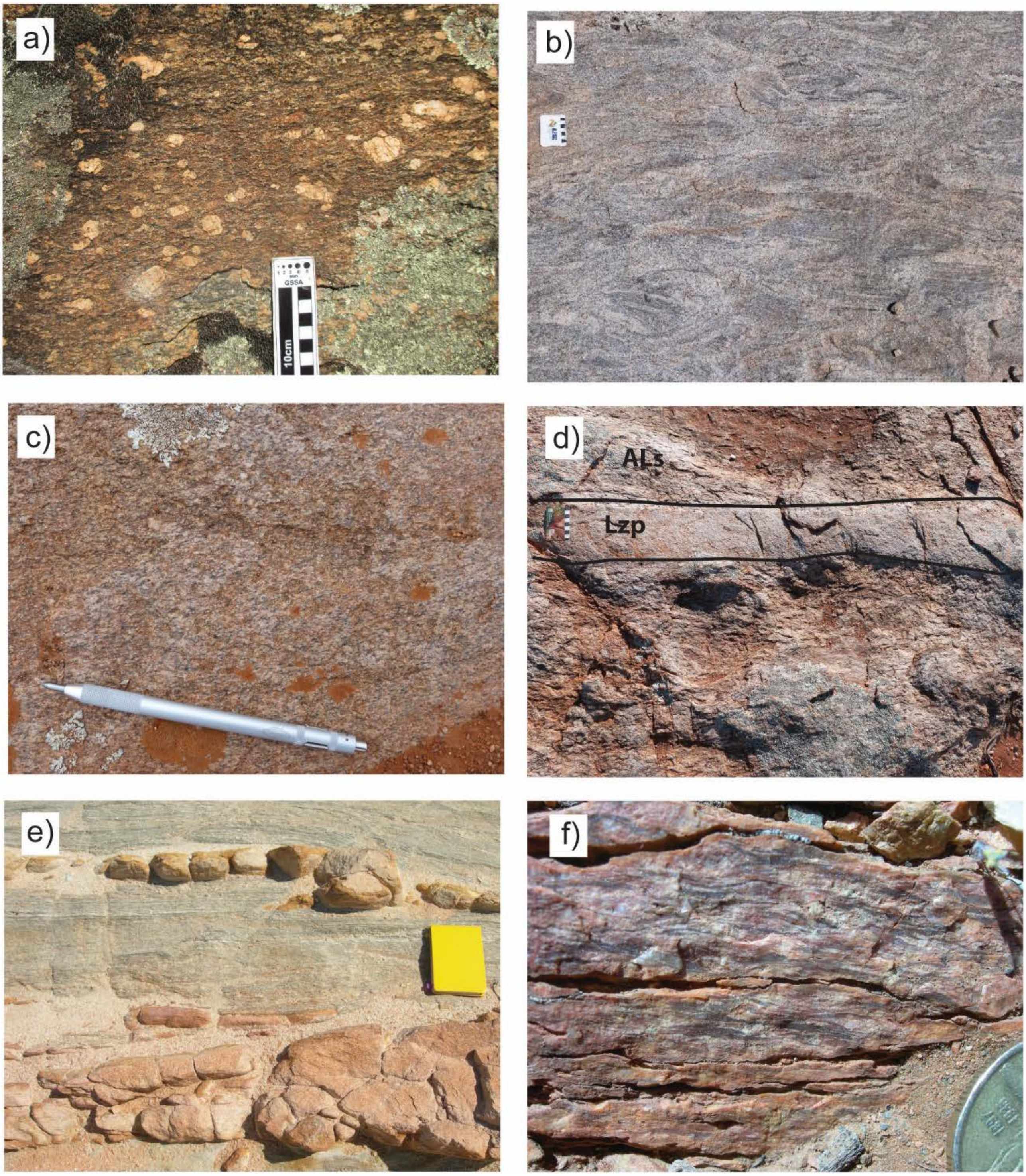

Figure 7. Sleaford Complex on northern Eyre Peninsula. (a) K-feldspar augen gneiss, salt lakes northeast of Pondanna Rock (site 2015281). **(b)** Quartz-plagioclase-K-feldspar-biotite-garnet migmatite at Waddikee Rocks (site 1993647). **(c)** Sparsely porphyritic foliated quartz-feldspar-biotite granite, western limb of Peter Pan syncline (site 2015853). **(d)** Granitic gneiss of Sleaford Complex intruded by fine-grained granite of the Peter Pan Supersuite, Peter Pan Platforms (site 1993650). **(e)** Leucogranite intruding sheared quartzofeldspathic paragneiss. The leucogranite is isoclinally folded, with the lower limb sheared out (photo 407568). **(f)** Dextral shear fabric within foliated leucogranite, northern shore of Lake Gilles (photo 407569).

TEMPORAL EQUIVALENTS TO THE SLEAFORD COMPLEX AT BRATTEN CAIRN

Felsic and mafic orthogneiss and paragneiss at Bratten Cairn (Fig. 3), north of Port Neill on eastern Eyre Peninsula, is also correlated with the Sleaford Complex (Schwarz, 2003). These rocks lie within the Kalinjala Shear Zone, and were subject to high-temperature metamorphism during the Kimban Orogeny (Hand *et al.*, 2012) . Metasediments comprise quartzofeldspathic metasediment, garnet-orthopyroxene-granulite, garnet-magnetite-ironstone and calc-silicate, which are interleaved with orthogneiss including grey granite gneiss, K-feldspar rich granitic gneiss, quartz-plagioclase-biotite-K-feldspar-garnet migmatitic orthogneiss (Fig. 8a) and pyroxene-plagioclase-quartz gneiss (Fig. 8b; Hand *et al.*, 2012). Migmatitic orthogneiss has yielded a magmatic crystallisation age of 2427 ±7 Ma, and mafic gneiss a magmatic crystallisation age of 2504 ± 6 Ma (Hand *et al.*, 2012).

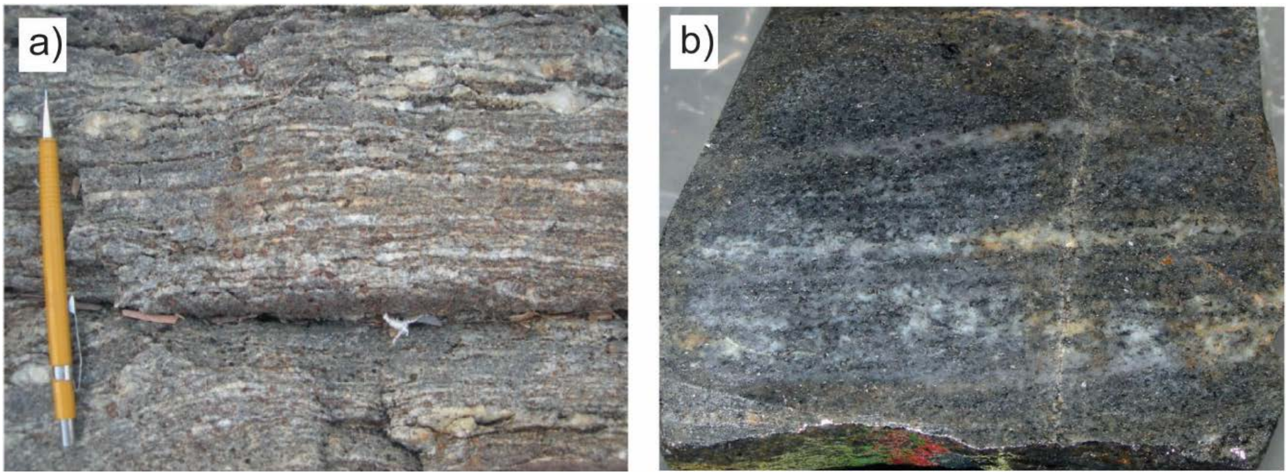

Figure 8. Sleaford Complex equivalents at Bratten Cairn. (a) quartz-plagioclase-biotite-K-feldspar-garnet migmatite (site 1773422). **(b)** Orthopyroxene-clinopyroxene-plagioclase-quartz mafic gneiss (site 1773438).

MINBRIE GNEISS

The Minbrie Gneiss occurs in the Cleve Hills as a northeast- to north-trending curvilinear belt, ~95 km long and ~3 km wide at its southern end, widening to ~25 km in the north (Fig. 3). It has an inferred structural contact with the Coolanie Gneiss, is structurally interleaved with the Hutchison Group and intruded by the 1735 Ma Middle Camp Granite (Parker & Fanning, 1998; Fraser & Neumann, 2010).

The Minbrie Gneiss is a composite stratigraphic unit that comprises a range of lithologies, including granitic gneiss, augen gneiss and quartz-feldspar-biotite migmatite granitic gneiss along with sills of amphibolite and pegmatite (Parker *et al.*, 1981). Granitic gneiss is medium-grained and equigranular, composed of quartz, plagioclase, K-feldspar and biotite, and is tonalitic to granodioritic in composition (Figs 9a & b; Parker *et al.*, 1981). Augen gneiss is composed of potassium feldspar augen wrapped by a foliated medium-grained biotite-quartz-feldspar matrix. Migmatite is heterogeneous (Figs 9c-f), and includes patch metatexite containing discontinuous leucosomes, net-structured metatexite containing leucosomes parallel to the gneissic fabric and in shear bands, and rafts of quartz-feldspar-biotite gneiss within leucosomes. Amphibolite sheets comprise green-brown hornblende and plagioclase, locally with minor orthopyroxene, and were emplaced prior to metamorphism of the Minbrie Gneiss (Parker *et al.*, 1981).

The Minbrie Gneiss was previously classified as part of the Lincoln Complex (1850–1690 Ma), and interpreted to have been derived from the migmatisation of the Sleaford Complex, Miltalie Gneiss and early-formed Kimban granites during the Kimban Orogeny (Parker, 1993). This interpretation is supported by whole rock Rb-Sr geochronology of the Minbrie Gneiss, which yielded ages ranging from >1800 Ma to c. 2300 Ma (Webb *et al.*, 1986). However, U-Pb zircon geochronology for orthogneiss within the Minbrie Gneiss indicates that although deformed during the Kimban Orogeny, the Minbrie Gneiss intruded during the Neoarchaean to earliest Palaeoproterozoic, equivalent in age to the Sleaford Complex. It has yielded magmatic protolith ages within the range 2521 Ma to 2418 Ma (Fraser & Neumann, 2010, Jagodzinski & McAvaney, 2016). This geochronology demonstrates that this unit is a composite of felsic igneous rocks, containing igneous units intruded at the same time as the sedimentary protoliths of the Wangary Gneiss and Carnot Gneiss were deposited and the Hall Bay Volcanics were emplaced, as well as younger igneous units intruded synchronous with the Sleafordian Orogeny (e.g. the Dutton Suite).

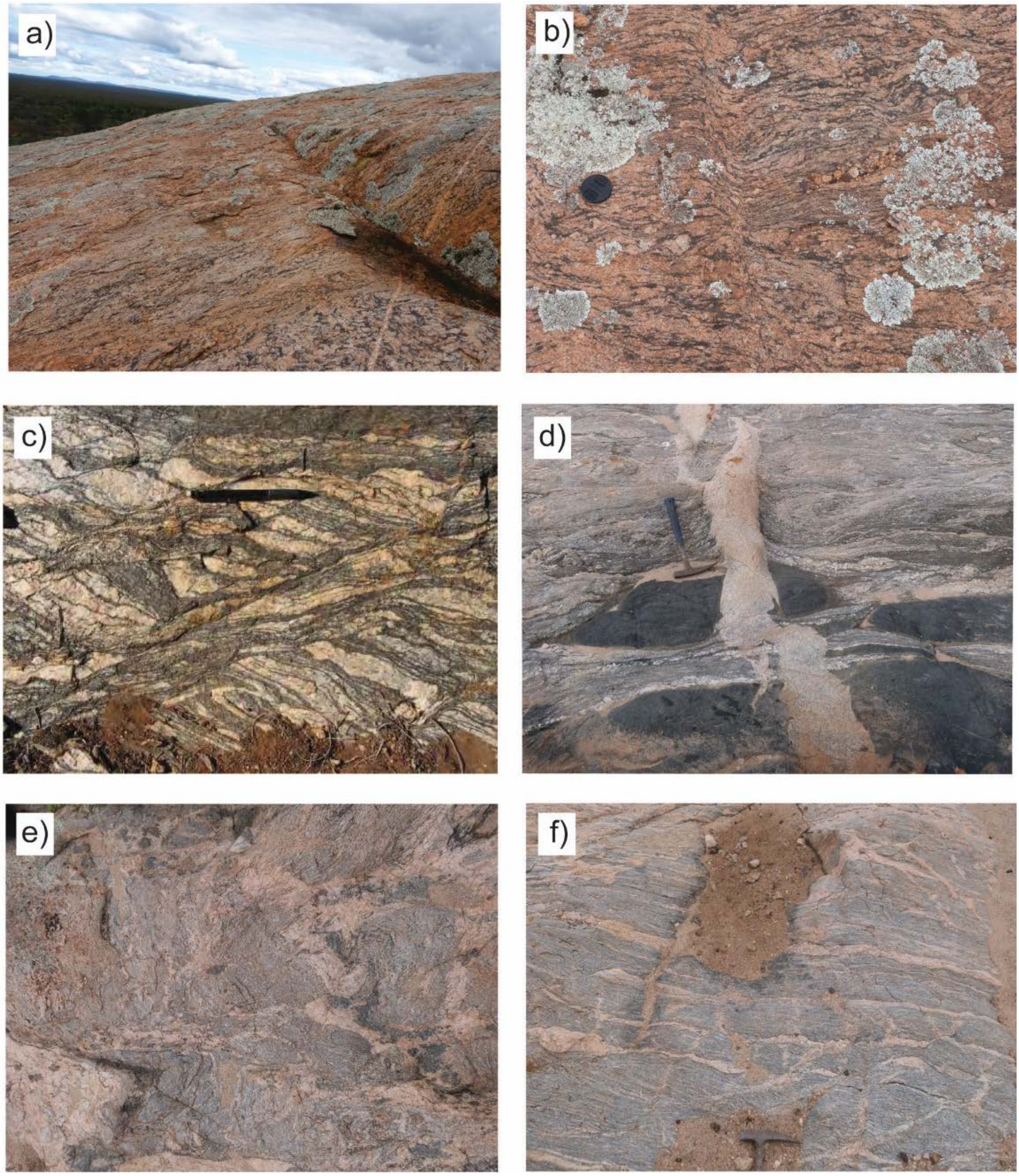

Figure 9. Lithologies of the Minbrie Gneiss. (a) Outcrop of Minbrie Gneiss, Secret Rocks (Refuge Rocks) (site 1993470). **(b)** Megacrystic K-feldspar-quartz-plagioclase-biotite gneiss, with fabric deflected by shear band. Looking W (site 1979800). **(c)** Banded migmatitic gneiss with K-feldspar-rich leucocratic layers and biotite-rich melanocratic layers displaced by shear bands with a sinistral shear sense, Mount Geharty (photo from Fraser & Neumann, 2010). **(d)** Quartz-feldspar-biotite migmatitic gneiss containing boudinaged amphibolite pods cross-cut by leucocratic dyke. Looking N Salt Creek. **(e)** Migmatite containing rafts of grey quartz-feldspar-biotite gneiss within leucosome, Salt Creek. **(f)** Net-structured metatextite migmatite containing leucosomes parallel to gneissic fabric and intruding shear bands, Salt Creek.

CARPA GRANITE

The Carpa Granite occurs as scattered outcrops in the Cleve Hills west of Cowell (Fig. 3). It is a massive, cream-pink, medium-grained, quartz-K-feldspar-plagioclase-biotite-muscovite granite to monzogranite with scattered aggregates of garnet (Parker *et al.*, 1981). It contains a sporadically developed foliation formed during the Kimban Orogeny, ranging from undeformed through to moderately foliated (Fig. 10).

The Carpa Granite was originally classified as part of the Lincoln Complex, and correlated with granites of the c. 1700 Ma Moody Suite on southern Eyre Peninsula due to its weak to sporadically developed fabric (Parker *et al.*, 1985). This interpretation was supported by a whole rock Rb-Sr age of 1677 ± 125 Ma (Webb *et al.*, 1986). Using a thermal ionisation mass spectrometry (TIMS) technique, Fanning (1987) later obtained a multigrain U-Pb zircon age of 1994 ± 27 Ma for the Carpa Granite, which was interpreted to reflect inherited zircon within a younger granite. However, recent SHRIMP zircon U-Pb dating from a sample of the Carpa Granite shows that the rock was emplaced at 2517± 7 Ma and contains minor c. 3400 Ma inheritance (Fraser & Neumann, 2010). The magmatic age of the Carpa Granite lies within the age range of the Sleaford Complex, similar in age to the Hall Bay Volcanics and Coulta Granodiorite. Notably, the SHRIMP analyses suggest some minor non-recent Pb loss, but do not record any evidence for zircon crystallisation during the Kimban Orogeny.

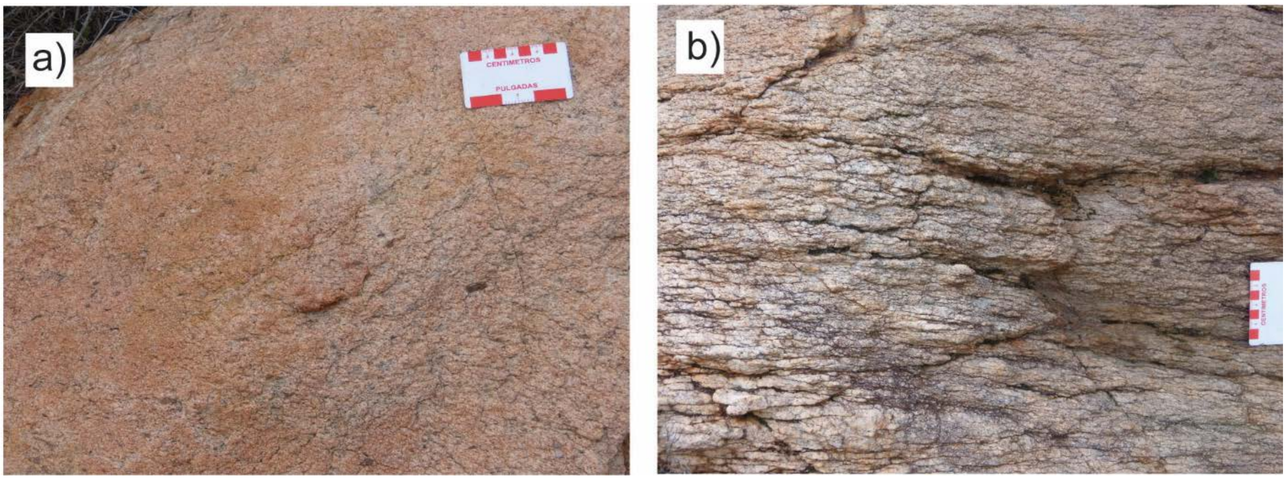

Figure 10. Carpa Granite. (a) Weakly foliated, fine-grained, quartz-feldspar-biotite-muscovite granite. **(b)** strongly foliated Carpa Granite.

ANALYTICAL METHODS AND DATA SOURCES

One Minbrie Gneiss sample and eight Carpa Granite samples were collected for major and trace element analyses (Fig. 11). The undifferentiated Minbrie Gneiss sample is a quartz-feldspar-biotite migmatite that was collected from Salt Creek, ~6.8 km northeast of Mount Geharty. This sample has a magmatic crystallisation age of c. 2420 Ma (Jagodzinski & McAvaney, 2016). The Carpa Granite samples were collected from a number of locations along the entire outcrop extent of the Carpa Granite in the Cleve Hills, extending from Carpa Homestead in the south to Middlecamp Station in the north. Lithologies sampled include massive, cream-pink, medium-grained, quartz-K-feldspar-plagioclase-biotite-muscovite granite and quartz-K-feldspar-plagioclase-biotite-muscovite-garnet granite

Major and trace element analyses were performed at two commercial geochemical laboratories in Adelaide (Amdel Laboratories and ALS Geochemistry Global), and are presented in Table 2. Major elements were analysed by Inductively Coupled Plasma with Optical Emission Spectroscopy (ICP-OES) at Amdel Laboratories and Inductively Coupled Plasma Mass Spectrometry (ICP-MS) at ALS Laboratories. All trace-elements were analysed by ICP-MS.

Existing geochemical analyses for the Minbrie Gneiss and Carpa Granite were collated from Webb *et al.* (1982), Stewart (1992), Neumann (2001) and SA_Geodata. Undifferentiated Sleaford Complex geochemical data was collated from Webb *et al*. (1982), Turner *et al.* (1993) and Swain *et al.* (2005).

Sm–Nd isotope analyses for one Minbrie Gneiss and two Carpa Granite samples were performed at the University of Adelaide following the method of Wade *et al.* (2006), and are presented in Table 3. Nd analyses were conducted using a Finnigan MAT 262 thermal ionization mass spectrometer, in static and quadruple-cup dynamic measurement modes, normalized to $^{146}/^{144}$Nd = 0.7219 and Nd concentrations corrected for 100 pg blank. Sm analyses were carried out on a Finnigan MAT 261 thermal ionisation mass spectrometer, in single-cup dynamic mode, and Sm concentrations were corrected for 50 pg blank. Existing Sm-Nd isotope analyses for Minbrie Gneiss and Carpa Granite were collated from Neumann (2001). Sm-Nd isotopes for undifferentiated Sleaford Complex and Mulgathing Complex were collated from Turner *et al.* (1993) and Swain *et al.* (2005). Age constraints for many of the samples analysed for Sm-Nd isotopes do not exist, so εNd and T_{DM} values were calculated at estimates of the age of these samples based on proximal dated samples.

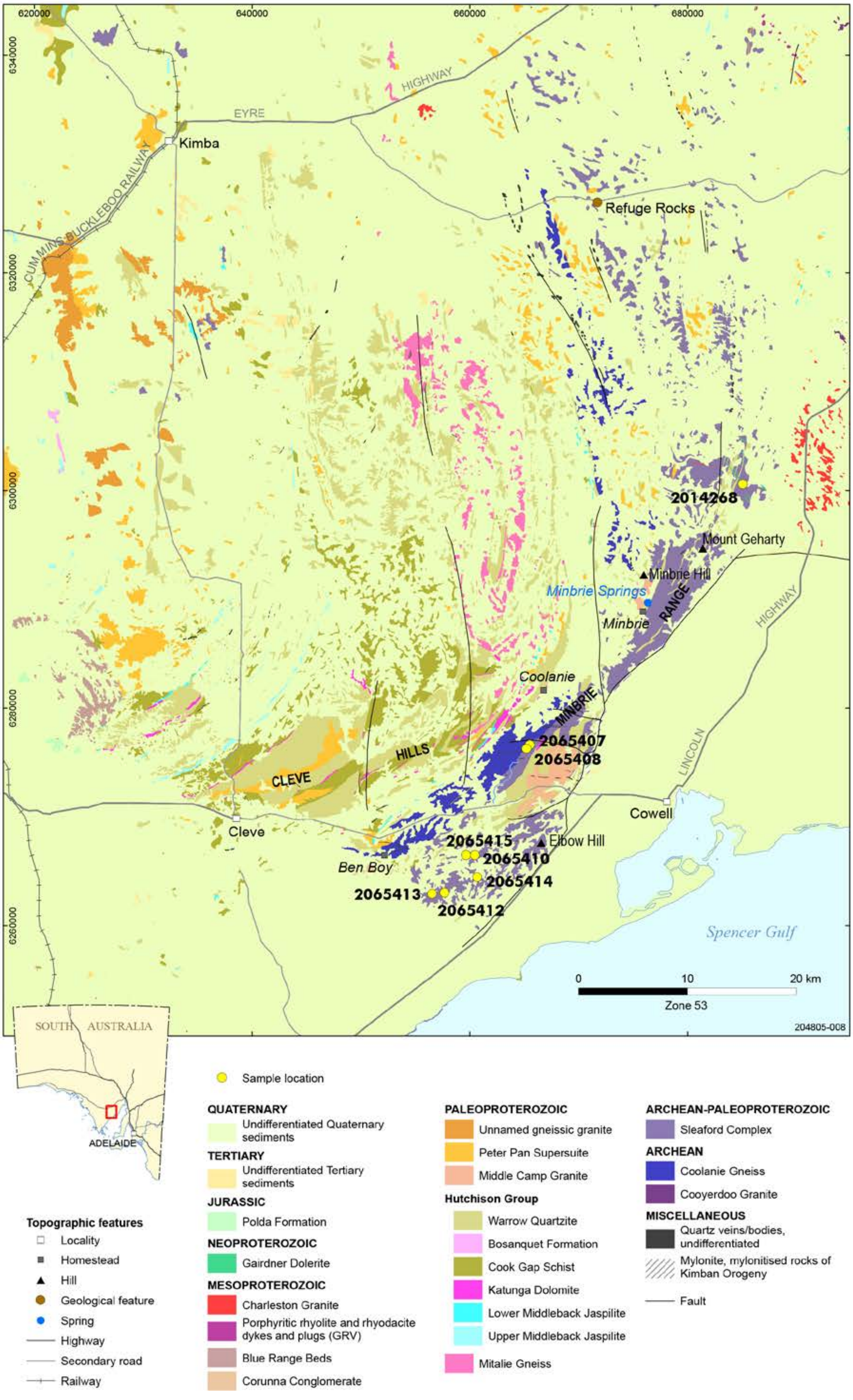

Figure 11. Location of samples of the Minbrie Gneiss and Carpa Granite collected in this study.

GEOCHEMISTRY

WHOLE ROCK GEOCHEMISTRY

Igneous protoliths of the Minbrie Gneiss are predominantly monzonite to granite in composition, with SiO_2 values ranging from ~53–75 wt% (Fig. 12a). The Minbrie Gneiss is classified as magnesian, calc-alkalic to alkali and peraluminous (Figs 12b-d). Major element abundances for the Minbrie Gneiss overlap with those of published data for igneous rocks of the Sleaford Complex, except that low silica Minbrie Gneiss have lower Fe_2O_3t (Fig. 13). Trace element abundances have a similar range to the undifferentiated Sleaford Complex (Fig. 13).

Compared to the Carpa Granite, the Minbrie Gneiss has a wider range of silica values and significant differences are seen in MgO (not shown), P_2O_5, U and Nb abundance (Fig. 13). The Minbrie Gneiss is characterised by negative Nb and Ti anomalies relative to primitive mantle composition, and is more enriched in high field strength and rare earth elements than the Carpa Granite (Fig. 14). The Minbrie Gneiss has moderate negative Eu anomalies and rare earth element (REE) abundance is similar to global subducting sediment (GLOSS) and plots completely within the REE range of the Sleaford Complex (Fig. 14).

The Carpa Granite displays many geochemical similarities to igneous rocks of the Sleaford Complex. The Carpa Granite is a high silica ($SiO_2 > 69$ wt%) granite (Fig. 12a), which plots predominantly within the magnesian field, and is alkali-calcic and peraluminous (Figs 12b-d). The Carpa Granite forms decreasing trends for major elements Al_2O_3, CaO, TiO_2 and Fe_2O_3t (Fig. 13). No clear trends are defined by trace elements shown on Figure 13. The Carpa Granite displays negative anomalies for Ba, Nb, Sr and Ti in primitive mantle normalised trace element plots (Fig. 14), with a similar trace element pattern to Sleaford Complex granites, and some samples display affinity to tonalite-trondhjemite-granodiorite (TTG) compositions. Rare earth element profiles are moderately flat, with slight enrichment in light REE (LREE) relative to heavy REE (HREE) and moderate negative Eu anomalies (Eu/Eu* = 0.19–0.38; Fig. 14).

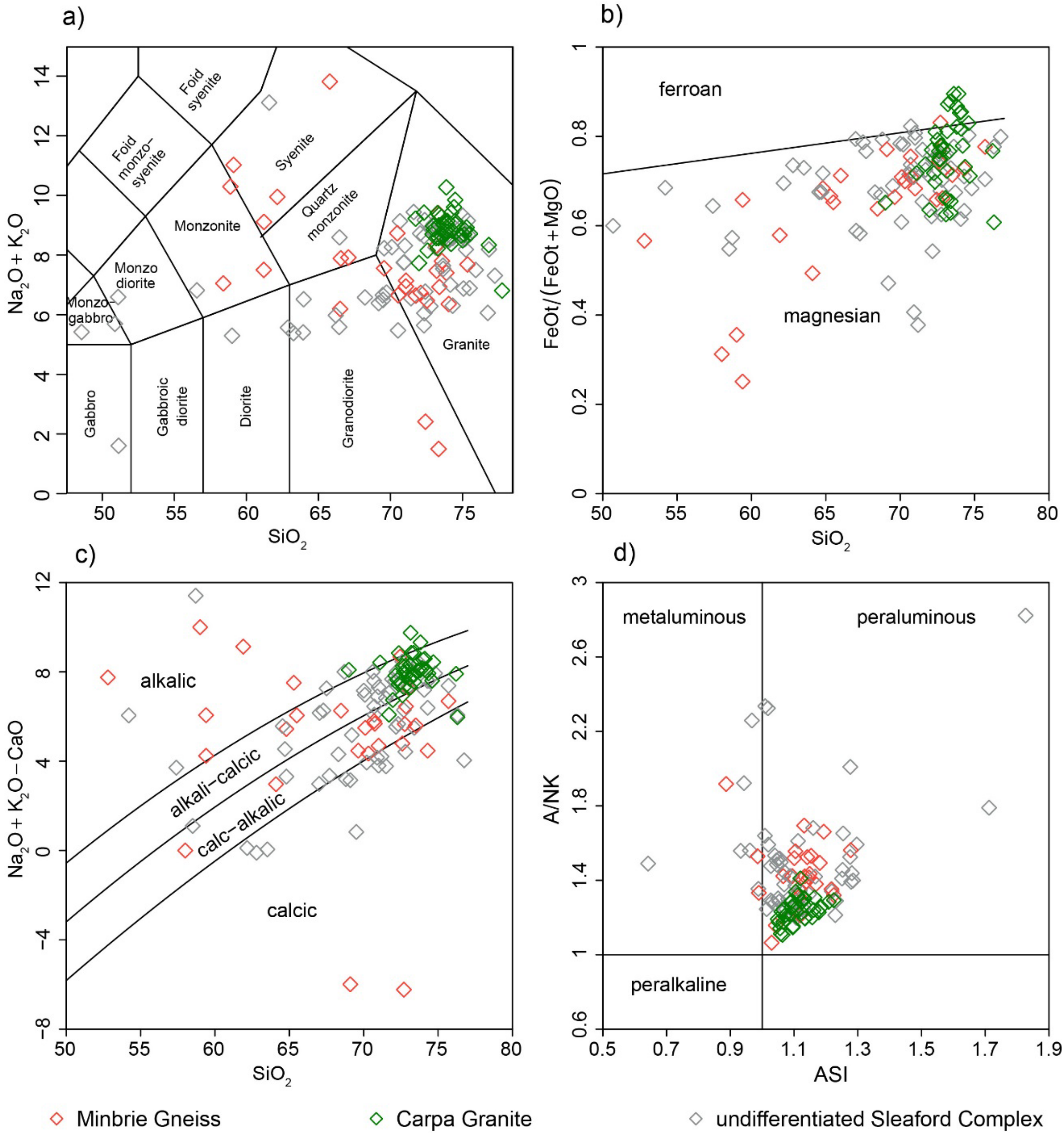

Figure 12. Classification diagrams for Minbrie Gneiss, Carpa Granite and Sleaford Complex. **(a)** Total alkali silica diagram. **(b)** Fe* [$FeO^{tot}/(FeO^{tot}$ + MgO)] diagram. **(c)** Modified alkali-lime index ($Na_2O + K_2O$ – CaO); **(d)** Aluminium Saturation Index Al/(Ca – 1.67P + Na +K).

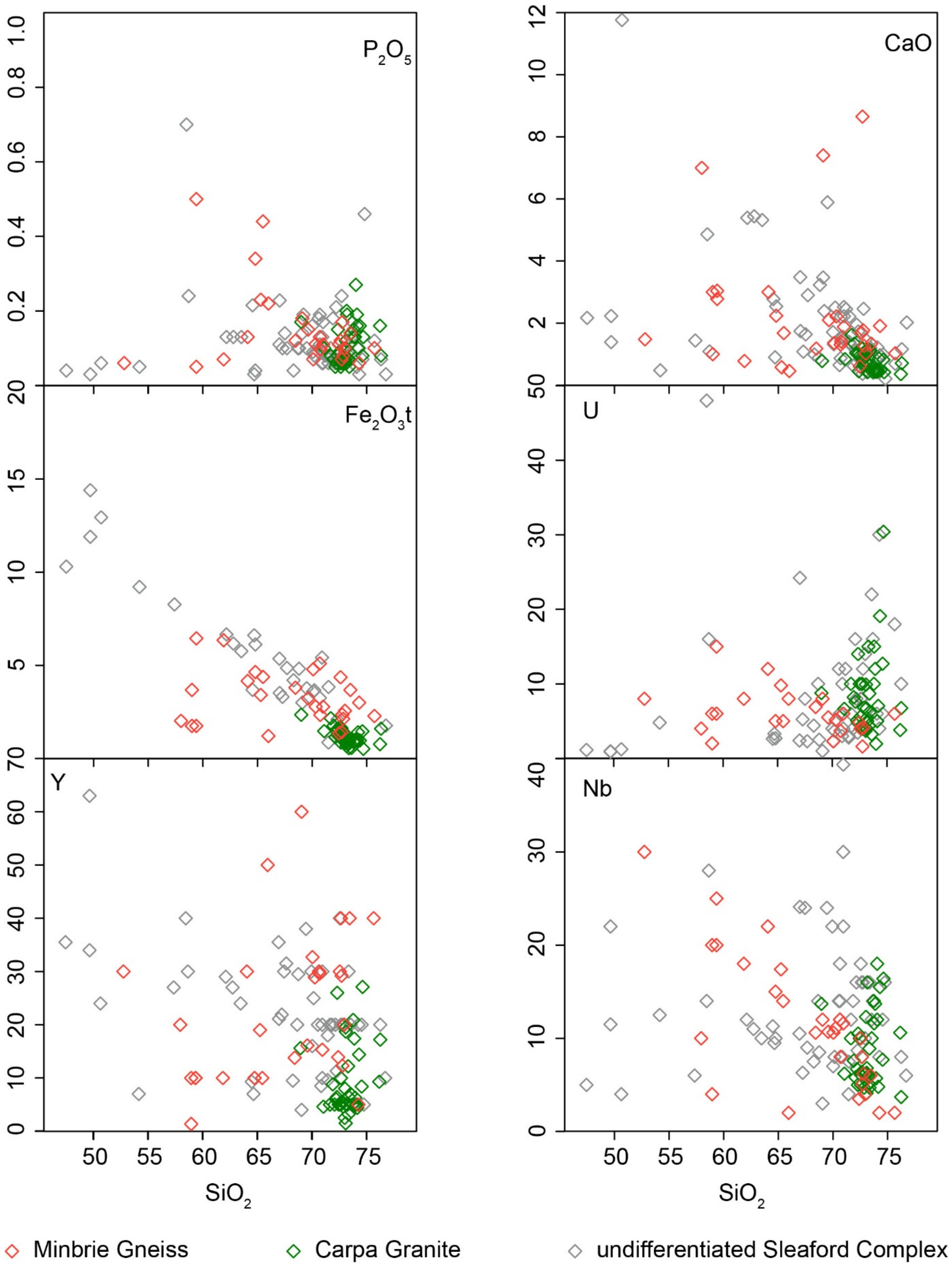

Figure 13. Selected major and trace element bivariate diagrams for Minbrie Gneiss and Carpa Granite, compared to the Sleaford Complex.

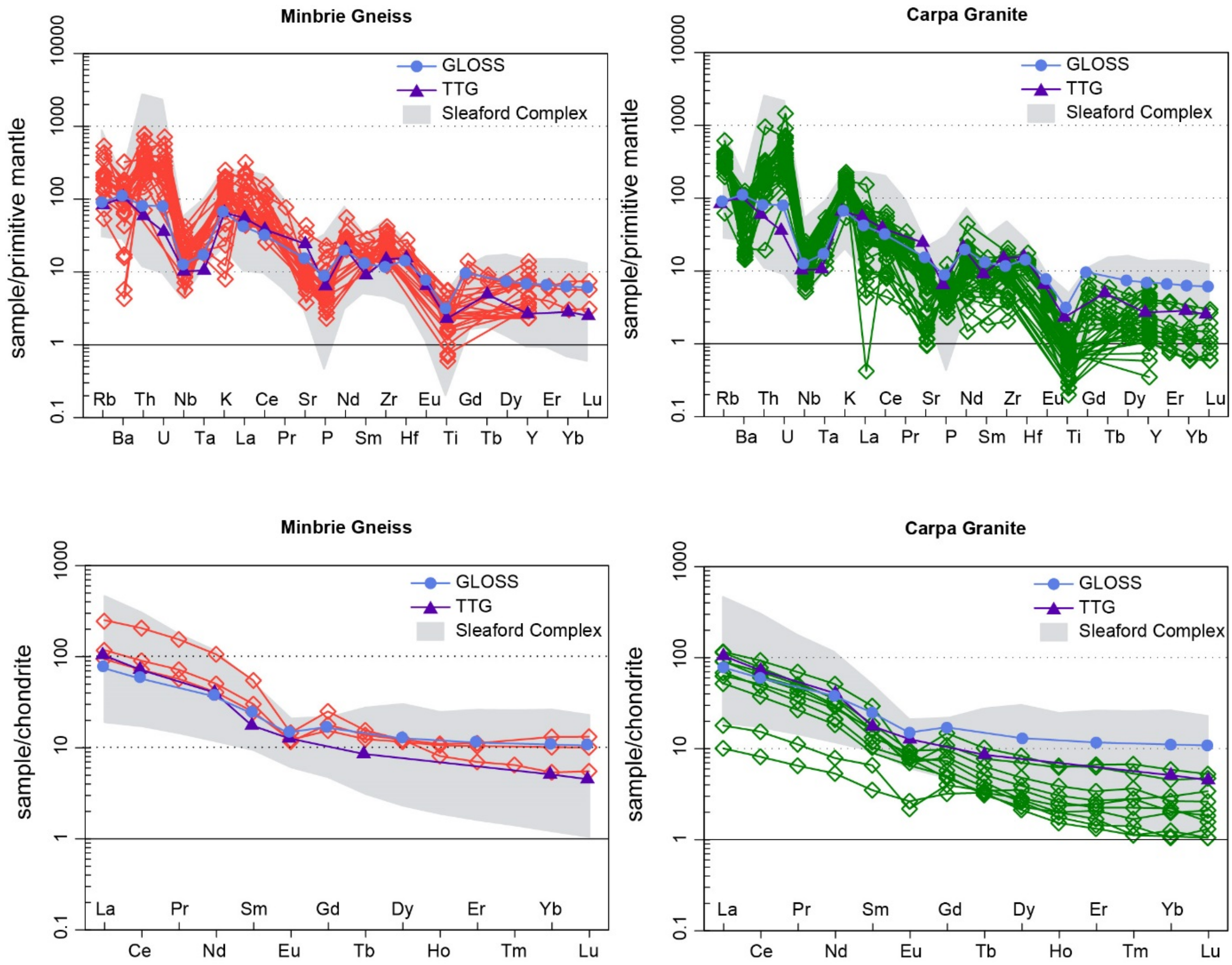

Figure 14. Trace element and REE plots for Minbrie Gneiss and Carpa Granite, compared to the Sleaford Complex.

Table 2. Whole rock geochemical data for eight Carpa Granite and one Minbrie Gneiss granite collected for this study.

Sample	**2065407**	**2065408**	**2065411**	**2065412**	**2065413**	**2065414**	**2065415**	**2065410**	**2014268**
Suite	Carpa Granite	Carpa Granite	Carpa Granite	Carpa Granite	Carpa Granite	Carpa Granite	Carpa Granite	Carpa Granite	Minbrie Gneiss
E	665521	665232	660692	657685	656549	659674	659674	660493	685090
N	6276620	6276257	6264442	6263023	6262914	6266468	6266468	6266474	6300552
Zone	53	53	53	53	53	53	53	53	53
Age (Ma)	2515	2515	2515	2515	2515	2515	2515	2515	2420
Lithology	granite	granite	granite	granite	granite	granite	granite	granite	migmatite
Major elements (wt%)									
SiO_2	74	73.6	72.8	72.7	72.6	69	76.3	71.1	65.30
TiO_2	0.04	0.05	0.16	0.19	0.22	0.33	0.13	0.19	0.58
Al_2O_3	14.5	14.15	14.55	15.1	14.85	13.75	11.85	14.95	13.25
Fe_2O_3T	1.03	0.57	1.46	1.61	1.68	2.35	1.6	1.47	3.41
MgO	0.16	0.06	0.37	0.41	0.46	1.13	0.93	0.52	1.54
MnO	0.02	0.01	0.02	0.02	0.02	0.03	0.02	0.02	0.02
CaO	0.43	0.44	0.64	0.82	1.2	0.78	0.71	0.84	0.58
Na_2O	4.2	5.47	3.93	4.22	4.33	3.7	5.06	3.98	2.28
K_2O	4.77	3.02	4.98	4.6	3.82	5.17	1.62	5.28	5.81
P_2O_5	0.27	0.14	0.06	0.06	0.06	0.17	0.08	0.1	0.23
L.O.I.	0.29	0.3	0.41	0.39	0.39	0.3	0.16	0.29	0.76
Trace and rare earth elements (ppm)									
Ga	19.1	20	21.5	21.7	22.4	21.3	14.5	20.2	21.00
Cr	<10	10	10	10	10	20	10	10	20.00
Ni	1	<1	3	1	1	11	6	5	5.00
Sc	3	2	2	2	2	5	2	2	7.00
Cu	<1	<1	2	<1	<1	4	12	<1	8.00
Zn	12	2	20	29	36	12	11	30	58.00
Sn	9	3	1	2	1	6	2	3	6.00
V	<5	<5	8	9	11	30	18	11	37.00
Y	6.3	7	5.6	10	5.1	15.6	17.2	4.6	19.00
Rb	227	141.5	191.5	181	159	159	39.4	201	241.00
Sr	38.40	58.30	157.00	194.50	226.00	104.00	57.70	208.00	222.00
Cs	6.22	0.84	1.22	1.66	2.24	0.99	0.61	4.2	2.30
Ba	142.5	124	629	752	738	530	109	872	1290.00
Th	1.64	6.64	10.65	14.7	26.8	25.4	16.55	13.95	66.00
U	1.96	3.22	3.98	4.46	5.62	8.77	6.75	6.64	9.79
Ta	2	1.3	0.6	0.5	0.6	1	0.4	0.9	1.10
Nb	5.7	10	5.2	6.4	6.1	13.7	3.7	6.2	17.40
Pb	17	30	39	41	37	22	20	42	48.00
Hf	1.1	1.4	2.6	3.4	4	5	3.9	3.1	7.80
Zr	23	35	87	114	142	174	123	106	274.00
La	3.7	6.6	19.2	33.2	41.7	42.6	23.3	25.6	92.50
Ce	7.8	14.7	35.9	66.9	74.4	88.9	48.9	46.2	197.00
Pr	0.89	1.53	3.65	6.96	7.28	9.52	5.27	4.53	21.20
Nd	3.8	5.6	13.1	25.9	24.9	36.4	19.6	15.6	75.60
Sm	0.81	1.52	2.08	4.3	3.72	6.78	3.79	2.38	12.65
Eu	0.23	0.19	0.57	0.83	0.68	0.72	0.58	0.67	1.27
Gd	0.98	1.22	1.54	2.99	2.25	4.52	3.33	1.46	7.66
Tb	0.19	0.2	0.18	0.37	0.25	0.59	0.45	0.19	0.90
Dy	1.09	1.34	0.88	1.83	1.05	3.17	2.67	0.81	4.67
Ho	0.2	0.22	0.17	0.33	0.17	0.55	0.53	0.13	0.69
Er	0.61	0.56	0.52	0.85	0.42	1.56	1.66	0.33	1.74
Tm	0.1	0.08	0.06	0.13	0.04	0.19	0.24	0.04	0.23
Yb	0.74	0.55	0.49	0.66	0.31	1.13	1.46	0.27	1.33
Lu	0.13	0.06	0.08	0.1	0.04	0.18	0.2	0.04	0.21

SM-ND ISOTOPE GEOCHEMISTRY

Sm-Nd isotope results for the Minbrie Gniess and Carpa Granite, compared to existing data for the Sleaford Complex, are presented in Table 3 and growth curves are displayed on Fig. 15. $\varepsilon_{Nd(t)}$ values for existing Nd data of the Minbrie Gneiss and Carpa Granite from Neumann (2001), originally calculated for magmatic crystallisation ages of 1850 Ma and 1700 Ma respectively, were recalculated based on the new geochronology for the Minbrie Gneiss and Carpa Granite of Fraser and Neumann (2010) (see Table 3).

$^{143}Nd/^{144}Nd$ ratios for the Minbrie Gneiss range from 0.510920–0.511364 and $^{147}Sm/^{144}Nd$ ratios from 0.0979–0.1200 (Table 3). The Minbrie Gneiss has a very narrow range of $\varepsilon_{Nd(2520\ Ma)}$ values between -1.5 and 0 with T_{DM} that range from 2.8–2.9 Ga. $^{143}Nd/^{144}Nd$ ratios for the Carpa Granite range from 0.511056–0.511733 and $^{147}Sm/^{144}Nd$ ratios are 0.0930–0.1602. The Carpa Granite has very broad $\varepsilon_{Nd(2520\ Ma)}$ values of -6.4 to 2.8 and T_{DM} ages that range from 3.2–2.6 Ga.

Nd isotope values for both the Minbrie Gneiss and Carpa Granite lie within the range of published values for the Sleaford Complex, which has $\varepsilon_{Nd(2520\ Ma)}$ values ranging from -7.5 to 0.5 (but are typically > -1.3) and $T_{(DM)}$ ages of 3.2–2.8 Ga (Table 3; Fig. 15). The Nd values are also similar to those of granites of the Mulgathing Complex, and have $^{143}Nd/^{144}Nd$ ratios that range from 0.510827–0.511566 and $^{147}Sm/^{144}Nd$ ratios that range from 0.0839–0.1392. $\varepsilon_{Nd(2500\ Ma)}$ values range from -5.4 to 1.2 with T_{DM} that range from 2.4–3.3 Ga (Cowley & Fanning, 1991, Turner *et al.*, 1993, Hoatson *et al.*, 2005, Swain *et al.*, 2005, Wade, 2012).

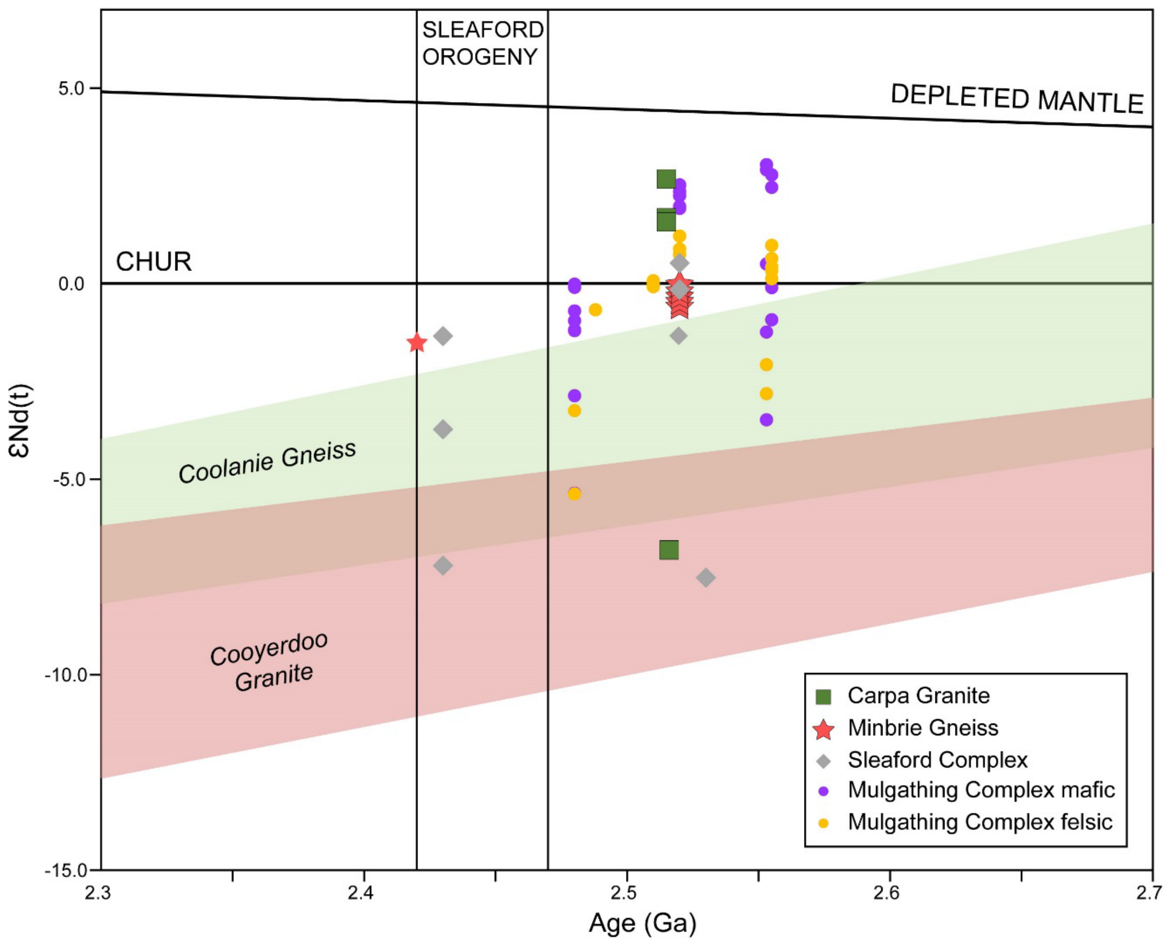

Figure 15. Nd evolution diagram for the Sleaford Complex and Mulgathing Complex. Average crustal evolution fields for the Mesoarchaean Cooyerdoo Granite and Coolanie Gneiss are also shown.

Table 3. Sm-Nd data for Sleaford Complex, including Carpa Granite and Minbrie Gneiss.

Sample	Unit	Lithology	E	N	Zone	Age (Ma)	Nd (ppm)	Sm (ppm)	$^{147}Sm/^{144}Nd$	$^{143}Nd/^{144}Nd$	$\varepsilon_{Nd(0)}$ [a]	$\varepsilon_{Nd(t)}$ [b]	$T_{(DM)}$	Reference
2014268	Minbrie Gneiss	migmatite	685089	6300552	53	2420	82.46	13.36	0.0979	0.510920	-33.5	-1.5	2.9	This paper
2065407	Carpa Granite	granite	665521	6276620	53	2520	3.74	0.99	0.1602	0.511706	-18.2	-6.4	3.2^	This paper
2065408	Carpa Granite	granite	665232	6276256	53	2520	5.50	1.43	0.1571	0.511733	-17.7	-4.9	3.1^	This paper
97CC-1	Minbrie Gneiss	granite	666400	6267600	53	2520	35.20	6.58	0.1132	0.511230	-27.5	-0.4	2.9	Neumann (2001)
97CC-25c	Minbrie Gneiss	granite	678220	6288285	53	2520	38.44	6.23	0.0982	0.510996	-32.0	-0.1	2.8	Neumann (2001)
97CC-26a	Minbrie Gneiss	granite	677230	6288650	53	2520	47.98	8.25	0.1041	0.511072	-30.5	-0.6	2.9	Neumann (2001)
97CC-4a	Minbrie Gneiss	granite	666370	6267700	53	2520	40.81	8.08	0.1200	0.511364	-24.8	0.0	2.9	Neumann (2001)
97CC-8	Minbrie Gneiss	granite	665450	6265220	53	2520	34.39	6.19	0.1089	0.511167	-28.7	-0.3	2.9	Neumann (2001)
97CC-65b	Carpa Granite	granite	665430	6270340	53	2520	17.74	2.72	0.0930	0.511056	-30.9	2.8	2.6	Neumann (2001)
97CC-11	Carpa Granite	granite	657980	6264500	53	2520	21.86	3.67	0.1015	0.511147	-29.1	1.7	2.7	Neumann (2001)
446/256	Undif. Sleaford Complex	granite	556600	6133000	53	2430	40.24	6.78	0.1020	0.510933	-33.3	-3.7	3.0	Turner *et al.* (1993)
466/C142	Undif. Sleaford Complex	granite	556600	6133000	53	2430	8.34	2.32	0.1685	0.511820	-16.0	-7.2	3.2^	Turner *et al.* (1993)
JC3	Undif. Sleaford Complex	granite	556600	6133000	53	2430	17.12	2.64	0.0934	0.510916	-33.6	-1.3	2.8	Turner *et al.* (1993)
621276	Undif. Sleaford Complex	granodiorite	523502	6220092	53	2520	27.89	5.83	0.1264	0.511498	-22.2	0.5	2.9	Swain *et al.* (2005)
621277	Undif. Sleaford Complex	granodiorite	523816	6219714	53	2520	26.08	5.86	0.1359	0.511621	-19.8	-0.2	3.0	Swain *et al.* (2005)
621279	Undif. Sleaford Complex	granodiorite	523365	6222587	53	2520	30.71	6.64	0.1308	0.511537	-21.5	-0.1	2.9	Swain *et al.* (2005)
1077-250	Undif. Sleaford Complex	granite	580950	6330090	53	2520	33.53	6.27	0.1132	0.511193	-28.2	-1.2	2.9	Stewart, unpublished
2008371081	Undif. Sleaford Complex	granite	675870	6384467	53	2530	46.13	6.62	0.0868	0.510423	-43.2	-7.5	3.2	OZ Chem

a $^{143}Nd/^{144}Nd$ CHUR(0) = 0.512638, $^{147}Sm/^{144}Nd$ CHUR(0) = 0.1966.
b T_{DM} calculated using the single stage model of Goldstein et al. (1984).
$\varepsilon_{Nd(T)}$ calculated at Age (Ma).
^ = 2-stage T_D

GEOCHEMICAL AND ISOTOPIC CONSTRAINTS ON SOURCE REGION AND TECTONIC SETTING

The geochemistry of the igneous units of the Sleaford Complex form three compositional groups, which differ in age: (i) juvenile igneous protoliths intruding before the onset of the Sleafordian Orogeny, (ii) evolved igneous protoliths intruding before the onset of the Sleafordian Orogeny, and (ii) evolved igneous protoliths intruding during the Sleafordian Orogeny.

JUVENILE IGNEOUS PROTOLITHS INTRUDING SYNCHRONOUS WITH SEDIMENTATION AND VOLCANISM, BEFORE THE ONSET OF THE SLEAFORDIAN OROGENY

Most samples of the Minbrie Gneiss (excluding sample 2014268), two samples of the Carpa Granite (97CC-65b and 97CC-11 from Neumann, 2001) and other igneous units of the Sleaford and Mulgathing complexes that intruded in the time period 2570–2470 Ma, prior to the Sleafordian Orogeny (c. 2470–2420 Ma) have a restricted range of juvenile isotopic signatures (Fig. 15), indicating a juvenile crustal source region. Juvenile crust may be formed in two broad tectonic settings: in rift-zones or at convergent margins.

Granites formed in rift-related settings are characterised by ferroan and alkali-calcic compositions, high Ga/Al ratios, elevated high field strength elements (HFSE), and high Fe and Ti contents (Manair & Piccoli, 1989; Eby, 1992). The Minbrie Gneiss is magnesian in composition (Fig. 12), and while some enrichment in HFSE is observed (Fig. 14), Ga/Al ratios are not high (Fig. 16; 10000*Ga/Al <3), which does not support a mantle-derived rift-related origin for this unit. While the Carpa Granite is predominantly alkali-calcic in composition (Fig. 12), it is also mostly magnesian, and HFSE such as Zr+Nb+Ce+Y values, and Ga/Al ratios are not elevated (Fig. 16). These attributes also do not support a rift-related origin.

In convergent margin settings granites are characterised by juvenile isotopic signatures, and depletions in HFSE such as Nb, Ta, Zr, Hf and Ti relative to large ion lithophile elements (LILE) and rare earth elements (REE; Pearce & Peate, 1995; Stolz *et al.*, 1996; Eiler *et al.*, 1998; Foley *et al.*, 2002; Münker *et al.*, 2004). The depletions are attributed to processes from the subducting slab-mantle wedge interface where the mantle wedge is enriched in fluids and melts from subducted oceanic crust and overlying sediments (Ringwood, 1974, Plank & Langmuir, 1998). Depletions in Nb and Ti are also characteristic of continental crust, and may be indicative of crustal contamination (Plank & Langmuir, 1998; Barth *et al.*, 2000; Rudnick & Gao, 2003), often coupled with evolved isotopic signatures and old model ages.

Trace element patterns of the Minbrie Gneiss and Carpa Granite are characterised by negative Nb and Ti anomalies (Fig. 14), which may be indicative of a subduction-related convergent margin setting (Pearce & Peate, 1995; Stolz *et al.*, 1996; Eiler *et al.*, 1998; Foley *et al.*, 2002) and/or crustal contamination. The juvenile Nd signatures of these units suggest contamination by older crustal material did not play a significant role in the formation of the granites. Hence, given the juvenile isotopic nature of the Minbrie Gneiss and Carpa Granite and close geochemical affinities to GLOSS on trace element and REE diagrams (Fig. 14), a subduction-related convergent margin setting is the preferred interpretation for the tectonic setting of these units.

The Minbrie Gneiss is a peraluminous quartz-feldspar-biotite gneiss and largely corresponds to S-type granites of Chappell and White (1974), representing crustal-derived melts. Major element and trace element geochemistry (e.g. low $CaO/(FeO+MgO+TiO_2)$, variable $CaO+FeO+MgO+TiO_2$, Sr/Y <30) suggest the Minbrie Gneiss was derived at shallow crustal levels, possibly intruded as shallow batholiths (Patiño Douce, 1999). Geochemically and isotopically, the Minbrie Gneiss is similar to other igneous units of the Sleaford Complex on southern Eyre Peninsula, suggesting a similar source region.

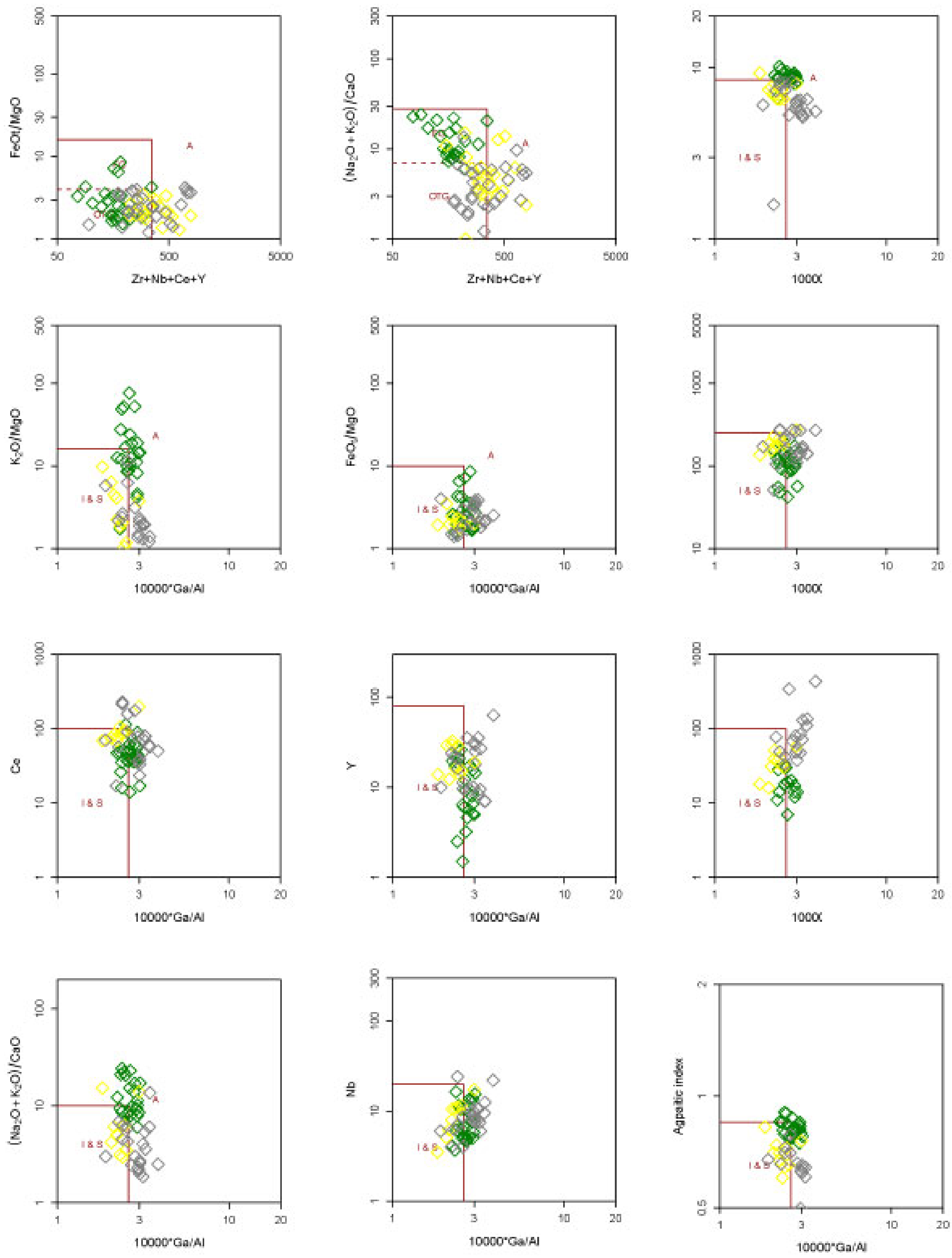

Figure 16. Discrimination diagrams of Whalen et al. (1987), showing the fields of A-type versus I- & S-type granites.

The Carpa Granite comprises a quartz-K-feldspar-plagioclase-biotite-muscovite±garnet granite which also resembles crustal-derived melts of Chappell and White (1974). While largely similar to other felsic igneous units of the Sleaford Complex, the Carpa Granite is characterised by higher silica contents (Fig. 12). It is also distinctly alkali-calcic (enriched in total alkalis) (Fig. 12), with relative depletions in Al_2O_3 and CaO and restricted Al_2O_3+FeO+MgO+TiO_2 contents. These characteristics have been attributed to peraluminous leucogranites derived from a mica-rich melt (Patiño Douce, 1999). As mica is consumed in dehydration melting, refractory minerals such as pyroxene, garnet and plagioclase dominate the melt (Patiño Douce, 1999).

EVOLVED IGNEOUS PROTOLITHS INTRUDING BEFORE THE ONSET OF THE SLEAFORDIAN OROGENY

Two samples of Carpa Granite, from the Narridy Creek area, have a considerably evolved isotopic signature ($\varepsilon_{Nd(2520\ Ma)}$ = -4.9 and -6.4; Fig. 15), which is coupled with a very old model age (4.6 Ga) indicating the incorporation of older, evolved continental crust. Only one other Sleaford Complex granite that was intruded pre-Sleafordian Orogeny, from the northern shore of Lake Gilles, has an evolved isotopic signature ($\varepsilon_{Nd(2530\ Ma)}$ = -7.5; T_{DM} = 3.2 Ga), suggesting the localised incorporation of older, evolved crustal material in these two locations (Fraser & Neumann, 2010). In the instance of the Lake Gilles sample, the Mesorchaean Cooyerdoo Granite crops out ~17 km to the southeast of this sample location, so it is reasonable to conclude that this sample has assimilated such basement material. Similarly, the Carpa Granite at Narridy Creek occurs proximal to the Mesoarchaean Coolanie Gneiss, and the isotopic data suggests that the Carpa Granite has assimilated Coolanie Gneiss or that the Coolanie Gneiss exists at depth in the source region from which the Carpa Granite was derived.

EVOLVED IGNEOUS PROTOLITHS INTRUDING DURING THE SLEAFORDIAN OROGENY

Igneous units of the Sleaford Complex that intruded during the Sleafordian Orogeny, which includes the Dutton Suite, some parts of the Minbrie Gneiss (sample 2014268), and the samples collected by Turner et al. (1993) from Cape Carnot, display a different isotopic character to the pre-deformational granites (>2470 Ma). These granites are isotopically more juvenile, with $\varepsilon_{Nd(2430\ Ma)}$ ranging from -7.2 to -1.3 (Fig. 15). There is an obvious negative trend in the isotopic evolution of the Sleaford and Mulgathing complex granites with decreasing age, indicating that leading up to and during orogenesis older and evolved crust was recycled or reworked into the system.

MODEL FOR THE TECTONIC SETTING AND EVOLUTION OF THE SLEAFORD AND MULGATHING COMPLEXES

The new data on the Minbrie Gneiss and Carpa Granite presented in this report are consistent with the existing models for tectonic setting and evolution of the Sleaford and Mulgathing Complexes presenting by Swain et al. (2005) and Reid et al. (2014). These models can be extended to incorporate the new data, as below:

(i) A volcano-sedimentary basin developed in a back-arc or arc-rift setting, accommodating eruption of the Devil's Playground Volcanics and Hall Bay Volcanics c. 2560–2520 Ma,

(ii) Deposition of sediments was synchronous with volcanism, including the protoliths of the Christie Gneiss, Kenella Paragneiss and parts of the Carnot Gneiss and Wangary Gneiss, and continued up until c. 2480 Ma.

(iii) The Lake Harris Komatiite erupted within the arc system at c. 2520 Ma by upwelling of a mantle-plume.

(iv) Juvenile crustal melts intruded the basin synchronous with volcanism and sedimentation, comprising the c. 2520 Ma Coulta Granodiorite, c. 2510 Ma Glenloth Granite, some parts of the Minbrie Gneiss, and some parts of the c. 2520 Ma Carpa Granite.

(v) At the same time, evolved crustal melts intruded the basin synchronous with volcanism and sedimentation, comprising the c. 2520 Ma Carpa Granite at Narridy Creek and the c. 2530 Ma Sleaford Complex on the northern shore of Lake Gilles.

(vi) Sedimentation and magmatism continued right up until the onset of the c. 2470–2420 Ma Sleafordian Orogeny, as evidenced by c. 2820 Ma maximum depositional ages of the Christie Gneiss and igneous rocks in the Mulgathing Complex. Evolved crustal melts intruded synchronous with deformation, including the Dutton Suite, parts of the Carnot Gneiss and the c. 2420 Ma Minbrie Gneiss from Salt Creek.

SUMMARY

Recent geochronology from the Minbrie Gneiss and Carpa Granite indicate that these units are part of the Neoarchaean to earliest Palaeoproterozoic Sleaford Complex rather than the Palaeoproterozoic Lincoln Complex. The geochemical signatures of the Minbrie Gneiss and Carpa Granite are also comparable to published data for igneous units of the Sleaford Complex. The Minbrie Gneiss and Carpa Granite represent both crustal reworking and the addition of new crustal material between 2520–2420 Ma. The Minbrie Gneiss has a juvenile and very narrow range of $\varepsilon_{Nd(2520\ Ma)}$ values between -1.5 and 0 with T_{DM} that range from 2.8–2.9 Ga which likely corresponds to remelting a source region similar to the earliest Neoarchaean basement. The Carpa Granite has a very broad range of $\varepsilon_{Nd(2520\ Ma)}$ values (-6.4 to 2.8) and T_{DM} ages that range from 3.2–2.6 Ga. This large variation is suggestive of a heterogeneous source region that includes new crustal material generating the juvenile Carpa Granite with positive Nd values (1.7 to 2.7), and an evolved Carpa Granite with negative Nd values (-4.9 to -6.8) derived from reworking of Mesoarchaean basement. Geochemical and mineralogical characteristics of the Minbrie Gneiss and Carpa Granite are consistent with the interpreted convergent margin setting of Swain et al. (2005).

ACKNOWLEDGEMENTS

Anthony Reid and Mark Pawley, Geological Survey of South Australia, are thanked for their reviews which greatly improved this manuscript. David Bruce, University of Adelaide, is thanked for carrying out the Sm–Nd isotope analysis.

REFERENCES

Allen, S. R., McPhie, J., Ferris, G. & Simpson, C. 2008. Evolution and architecture of a large felsic igneous province in western Laurentia: The 1.6 Ga Gawler Range Volcanics, South Australia. *Journal of Volcanology and Geothermal Research*, 172, pp. 132-147.

Barth, M., McDonough, W. F. & Rudnick, R. L. 2000. Tracking the budget of Nb and Ta in the continental crust. *Chemical Geology*, 165, pp. 197–213.

Bradley, G. M., 1972. The geochemistry of a medium pressure granulite terrain at southern Eyre Peninsula, Australia. Thesis, Australian National University, Canberra.

Chalmers, N., 2009. Geodynamic evolution of the St Peter Suite, Gawler Craton, South Australia: stratigraphic, geochemical and isotopic investigation. BSc Masters Thesis, Monash University,

Chappell, B. W. & White, A. J. R. 1974. Two contrasting granite types. *Pacific Geology*, 8, pp. 173–174.

Cowley, W. M., Conor, C. & Zang, W., 2003. New and revised Proterozoic stratigraphic units on northern Yorke Peninsula. *MESA Journal*, 29, pp. 46-58. Department of Primary Industries and Resources, South Australia, Adelaide.

Cowley, W. M. & Fanning, C. M. 1991. Low-grade Archaean metavolcanics in the northern Gawler Craton. *South Australia. Geological Survey. Quarterly Geological Notes*, 119, pp. 2-17.

Daly, S. & Fanning, C. M. 1993. Archaean. In Drexel, J. F., Preiss, V. W. & Parker, A. J. (Eds.), *The Geology of South Australia. Vol. 1, The Precambrian,* Bulletin 54. Geological Survey of South Australia, pp.33–50.

Daly, S. J. 1993. Tarcoola Formation. In Drexel, J. F., Preiss, W. V. & Parker, A. J. (Eds.), *The geology of South Australia. Vol 1, The Precambrian,* Bulletin 54*.* Geological Survey of South Australia, pp 68–69.

Daly, S. J., Fanning, C. M. & Fairclough, M. C. 1998. Tectonic evolution and exploration potential of the Gawler Craton, South Australia. *AGSO Journal of Australian Geology and Geophysics*, 17, pp. 145-168.

Dutch, R., 2009. Reworking the Gawler Craton: metamorphic and geochronologic constraints on Palaeoproterozoic rezctivation of the southern Gawler Craton, Australia. PhD. Thesis, Department of Geology and Geophysics, University of Adelaide, Adelaide.

Dutch, R., Hand, M. & Kelsey, D. E. 2010. Unravelling the tectonothermal evolution of reworked Archean granulite facies metapelites using in situ geochronology: an example from the Gawler Craton, Australia. *Journal of Metamorphic Geology*, 28, pp. 293-316.

Dutch, R., Hand, M. & Kinny, P. D. 2008. High-grade Palaeoproterozoic reworking in the southeastern Gawler Craton, South Australia. *Australian Journal of Earth Sciences*, 55, pp. 1063-1081.

Eby, G. N. 1992. Chemical subdivision of the A-type granitoids: Petrogenetic and tectonic implications. *Geology*, 20, pp. 641–644.

Eiler, J. M., McInnes, B., Valley, J., Graham, C. M. & Stopler, E. M. 1998. Oxygen isotope evidence for slab-derived fluids in the sub-arc mantle. *Nature*, 393, pp. 777–781.

Fanning, C. M. 1987. U-Pb geochronology of Broadview DDH 1, Wangary Gneiss, Carpa Granite and Middle Camp Granite. Amdel report G7155/88 (unpublished).

Fanning, C. M., Oliver, R. L. & Cooper, J. A. 1981. The Carnot Gneisses, southernmost Eyre Peninsula. *South Australia Geological Survey Quarterly Geological Notes*, 80, pp. 7-12.

Fanning, C. M., Reid, A. J. & Teale, G. S., 2007. *A Geochronological Framework for the Gawler Craton, South Australia*, Bulletin 55, Primary Industries and Resources, South Australia, Adelaide.

Flint, R. B. & Rankin, L. R., 1991. KIMBA Map Sheet, SI 53-7, Explanatory Notes. *South Australia Geological Atlas, 1:250 000 series*.

Foley, S., Tiepolo, M. & Vannucci, R. 2002. Growth of early continental crust controlled by melting of amphibolite in subduction zones. *Nature*, 417, pp. 837–840.

Fraser, G. & Lyons, P. 2006. Timing of Mesoproterozoic tectonic activity in the north-western Gawler Craton constrained by $^{40}Ar/^{39}Ar$ geochronology. *Precambrian Research*, 151, pp. 160-184.

Fraser, G., McAvaney, S., Neumann, N., Szpunar, M. & Reid, A. 2010. Discovery of early Mesoarchaean crust in the eastern Gawler Craton, South Australia. *Precambrian Research*, 179, pp. 1-21.

Fraser, G. & Neumann, N., 2010. New SHRIMP U-Pb zircon ages from the Gawler Craton and Curnamona Province, South Australia, 2008 - 2010. Geoscience Australia 2010/16.

Fraser, G., Reid, A. J. & Stern, R. A. 2012. Timing of deformation and exhumation across the Karari Shear Zone, north-western Gawler Craton, South Australia. *Australian Journal of Earth Sciences*, 59, pp. 1-24.

Goldstein, S. L., O'Nions, R. K. & Hamilton, P. J. 1984. A Sm-Nd isotopic study of atmospheric dusts and particulates from major river systems. *Earth and Planetary Science Letters*, 70, pp. 221-236. http://dx.doi.org/10.1016/0012-821X(84)90007-4

Halpin, J. A. & Reid, A. J. 2016. Earliest Paleoproterozoic high-grade metamorphism and orogenesis in the Gawler Craton, South Australia: The southern cousin in the Rae family? *Precambrian Research*, 276, pp. 123–144.

Hand, M., Reid, A., Dutch, R., Lane, K. & Jagodzinski, E. J., 2012, *Transpression and lower crustal extrusion: A transect across the Palaeoproterozoic Kalinjala Shear System in the southeastern Gawler Craton*. Report book 2012/00017, Department of Manufacturing, Innovation, Trade, Resources and Energy, South Australia, Adelaide.

Hand, M., Reid, A. J. & Jagodzinski. 2007. Tectonic framework and evolution of the Gawler Craton, South Australia. *Economic Geology*, 102, pp. 1377-1395.

Hoatson, D. M., Sun, S.-S., Duggan, M. B., Davies, M. B., Daly, S. J. & Purvis, A. C. 2005. Late Archaean Lake Harris Komatiite, central Gawler Craton, South Australia: geologic setting and geochemistry. *Economic Geology*, 100, pp. 349-374.

Hoek, J. D. & Schaefer, B. F. 1998. Palaeoproterozoic Kimban mobile belt, Eyre Peninsula: timing and significance of felsic and mafic magmatism and deformation. *Australian Journal of Earth Sciences*, 45, pp. 305-313.

Howard, K. E., Hand, M., Barovich, K., Payne, J. L. & Belousova, E. 2011a. U-Pb, Lu-Hf and Sm-Nd isotopic contstraints on provenance and depositional timing of metasedimentary rocks in the western Gawler Craton: implications for Proterozoic reconstruction models. *Precambrian Research*, 184, pp. 43-62.

Howard, K. E., Hand, M., Barovich, K., Payne, J. L., Cutts, K. A. & Belousova, E. 2011b. U-Pb zircon, zircon Hf and whole-rock Sm-Nd isotopic constraints on the evolution of Palaeoproterozoic rocks in the northern Gawler Craton. *Australian Journal of Earth Sciences*, 58, pp. 615-638.

Jagodzinski, E. & Reid, A. J., 2016, *U-Pb geochronological data from drill holes Nundroo 3 DDH and Nundroo 2 DDH, Fowler Domain, western Gawler Craton*. Report book 2016/00010, Department for State Development, Adelaide.

Jagodzinski, E. A., Black, L., Frew, R. A., Foudoulis, C., Reid, A., Payne, J. L., Zang, W. & Schwarz, M., 2006, *Compilation of SHRIMP U-Pb geochronological data for the Gawler Craton, South Australia 2005-2006*. Report book 2006/00020, Primary Industries and Resources South Australia, Adelaide.

Jagodzinski, E. A. & McAvaney, S. O., 2016, *SHRIMP U-Pb geochronology data for northern Eyre Peninsula, 2014 - 2015*. Report book 2016/00001, Department of State Development, South Australia, Adelaide.

Jagodzinski, E. A., Reid, A., Chalmers, N., Swain, G. M., Frew, R. A. & Foudoulis, C., 2007, *Compilation of SHRIMP U-Pb geochronological data for the Gawler Craton, South Australia, 2007*. Report book 2007/00021, Primary Industries and Resources South Australia, Adelaide.

Jagodzinski, E. A., Reid, A., Crowley, J., McAvaney, S. & Wade, C., 2016. Precise zircon U-Pb dating of a Mesoproterozoic silicic large igneous province: the Gawler Range Volcanics and Benagerie Volcanic Suite, South Australia., *Australian Earth Science Convention*, Geological Society of Australia, Adelaide, South Australia, oral presentation.

Jagodzinski, E. A., Reid, A. & Fraser, G., 2009, *Compilation of SHRIMP U-Pb geochronological data for the Mulgathing Complex, Gawler Craton, South Australia, 2007-2009*. Report book 2009/00016, Primary Industries and Resources South Australia, Adelaide.

Jagodzinski, E. A., Reid, A. J. & Hand, M., 2012, *SHRIMP U-Pb geochronology of Archaean to Palaeoproterozoic rocks from southern Eyre Peninsula*. Report book 2012/00015, Department of Manufacturing, Trade, Innovation, Resources and Energy, South Australia, Adelaide.

Lane, K., 2011. Metamorphic and geochronological constraints on the evolution of the Kalinjala Shear Zone, Eyre Peninsula. BSc. Hons. Thesis, Department of Geology and Geophysics, University of Adelaide, Adelaide.

Lane, K., Jagodzinski, E. A., Dutch, R., Reid, A. J. & Hand, M. 2015. Age constraints on the timing of iron ore mineralisation in the southeastern Gawler Craton. *Australian Journal of Earth Sciences*, 62, pp. 55–75.

Manair, P. D. & Piccoli, P. M. 1989. Tectonic discrimination of granitoids. *Geological Society of America Bulletin*, 101, pp. 635-643. 10.1130/0016-7606(1989)101<0635:TDOG>2.3.CO;2

McAvaney, S. 2012. The Cooyerdoo Granite: Palaeo- and Mesoarchaean basement of the Gawler Craton. *MESA Journal*, 65, pp. 31-40.

McAvaney, S. O. & Reid, A., 2008, *The Corunna Conglomerate, Gawler Craton: a review of the sedimentology and new U-Pb zircon geochronology*. Report book Report book 2008/003, Department of Primary Industries and Resources. South Australia, Adelaide.

McAvaney, S. O., Wade, C. E. & Jagodzinski, E. J., 2016. Tip Top and Wertigo granites, c. 1775 Ma magmatism on northeastern Eyre Peninsula. *MESA Journal*, 80, pp. 63-76. Department of State Development, South Australia, Adelaide.

McFarlane, C. R. M. 2006. Palaeoproterozoic evolution of the Challenger Au deposit, South Australia, from monazite geochronology *Journal of Metamorphic Geology*, 24, pp. 75-87.

McFarlane, C. R. M., Mavrogenes, J. A. & Tomkins, A. G. 2007. Recognizing hydrothermal alteration through a granulite facies metamorphic overprint at the challenger Au deposit, South Australia. *Chemical Geology*, 243, pp. 64-89.

Münker, C., Wörner, G., Yogodzinski, G. & Churikova, T. 2004. Behaviour of high field strength elements in subduction zones: constraints from Kamchatka–Aleutian arc lavas. *Earth and Planetary Science Letters*, 224, pp. 275–293.

Nebel, O., Nebel-Jacobsen, Y., Mezger, K. & Berndt, J. 2007. Initial Hf isotope compositions in magmatic zircon from early Proterozoic rocks from the Gawler Craton, Australia: a test for zircon model ages. *Chemical Geology*, 241, pp. 23-37.

Neumann, N., 2001. Geochemical and isotopic characteristics of South Australian Proterozoic granites: implications for the origin and evolution of high heat producing-terranes. PhD Thesis, Department of Geology and Geophysics, University of Adelaide, Adelaide.

Parker, A. J., 1978. Structural, stratigraphic and metamorphic geology of Lower Proterozoic rocks in the Cowell/Cleve district, eastern Eyre Peninsula. PhD Thesis, University of Adelaide, Adelaide.

Parker, A. J., 1980. The Kalinjala Mylonite Zone, eastern Eyre Peninsula. *Quaternary Geological Notes*, 76, pp. 6-11. Geological Survey of South Australia, Adelaide.

Parker, A. J., 1993. *Kimban Orogeny*, In J. F. Drexel, W. V. Preiss and A. J. Parker (Eds.), *The geology of South Australia, Volume 1, The Precambrian*, Bulletin 54. Geological Survey of South Australia, Adelaide. pp. 71-81.

Parker, A. J. & Fanning, C. M., 1998. WHYALLA Map Sheet, SI53-8, Explanatory Notes. *South Australia Geological Atlas 1:250 000 series*, Adelaide.

Parker, A. J., Fanning, C. M. & Flint, R. B. 1981. *Archaean-Middle Proterozoic geology of the southern Gawler Craton, South Australia*, Geological Survey South Australia, Adelaide.

Parker, A. J., Fanning, C. M. & Flint, R. B. 1985. Geology. In Twidale, C. R., Tyler, M. J. & Davies, M. (Eds.), *Natural History of Eyre Peninsula,* Royal Society of South Australia.

Parker, A. J., Fanning, C. M., Flint, R. B., Martin, A. R. & Rankin, L. R. 1988. *Archaean - Early Proterozoic Granitoids, Metasediments and Mylonites of Southern Eyre Peninsula, South Australia*, Specialist Group in Tectonics and Structural Geology, Geological Society of Australia Incorporated, Adelaide.

Parker, A. J. & Flint, R. B., 1983. WHYALLA Map Sheet, SI 53-8, *Geological Atlas of South Australia, 1:250 000 series*. Geological Survey of South Australia.

Patiño Douce, A. E. 1999. What do experiments tell us about the relaitve contributions of crust and mantle origin of granitic magma? In Castro, A., Fernandez, C. & Vigneresse, J. L. (Eds.), *Understanding granites: Integrating new and classical techniques,* Geological Society of London, Special Publications, pp 55–75.

Payne, J. L., Barovich, K. & Hand, M. 2006. Provenance of metasedimentary rocks in the northern Gawler Craton, Australia: Implications for Palaeoproterozoic reconstructions. *Precambrian Research*, 148, pp. 275-291.

Payne, J. L., Ferris, G., Barovich, K. M. & Hand, M. 2010. Pitfalls of classifying ancient magmatic suites with tectonic discrimination diagrams: An example from the Paleoproterozoic Tunkillia Suite, southern Australia. *Precambrian Research*, 177, pp. 227-240.

Pearce, J. A. & Peate, D. W. 1995. Tectonic implications of the composition of volcanic arc magmas. *Annual Review of Earth and Planetary Sciences*, 23, pp. 251–285.

Plank, T. & Langmuir, C. H. 1998. The chemical composition of subducting sediment and its consequences for the crust and mantle. *Chemical Geology*, 145, pp. 325-394.

Rankin, L. R., Flint, R. B. & Fanning, C. M., 1990, *Palaeoproterozoic Nuyts Volcanics of the western Gawler Craton*. Report book 90/00060, Deptartment of Primary Industries and Resources South Australia, Adelaide.

Reid, A. & Hand, M. 2012. Mesoarchaean to Mesoproterozoic evolution of the southern Gawler Craton, South Australia. *Episodes*, 35, pp. 216-225.

Reid, A., Hand, M., Jagodzinski, E. J., Kelsey, D. E. & Pearson, N. 2008a. Palaeoproterozoic orogenesis in the southeastern Gawler Craton, South Australia. *Australian Journal of Earth Sciences*, 55, pp. 449-471.

Reid, A. & Jagodzinski, E. A., 2011, *PACE Geochronology: Results of collaborative geochronology projects 2009-2010*. Report book 2011/003, Department of Primary Industries and Resources, South Australia, Adelaide.

Reid, A., Vassallo, J., Wilson, C. & Fanning, C. M., 2007, *Timing of the Kimban Orogeny on southern Eyre Peninsula*. Report book 2007/005, Department of Primary Industries and Resources, South Australia, Adelaide.

Reid, A. J., Jagodzinski, E. J., Fraser, G., L & Pawley, M. J. 2014. SHRIMP U-Pb age constraints on the tectonics of the Neoarchean to early Palaeoproterozoic transition within the Mulgathing Complex, Gawler Craton, South Australia. *Precambrian Research*, 250, pp. 27-49.

Reid, A. J., McAvaney, S. O. & Fraser, G. L. 2008b. Nature of the Kimban Orogeny across northern Eyre Peninsula. *MESA Journal*, 51, pp. 25-34.

Reid, A. J., Pawley, M. J., Jagodzinski, E. J. & Dutch, R. A., 2016, *Magmatic processes of the St Peter Suite, Gawler Craton: new U-Pb geochronological data and field observations*. Report book 2016/00012, Department of State Development, Adelaide.

Ringwood, A. E. 1974. The petrological evolution of island arc systems. *Journal of the Geological Society London*, 130 pp. 183–204.

Rudnick, R. L. & Gao, S. 2003. Composition of the continental crust. In Rudnick, R. L. (Ed.) *The Crust,* Elsevier/Pergamon, Oxford, pp 1-64.

Rutland, R. W. R., Parker, A. J., Pitt, G. M., Preiss, V. W. & B, M. 1981. The Precambrian of South Australia. In Hunter, D. R. (Ed.) *Precambrian of the Southern Hemisphere,* Developments in Precambrian Geology Series 2, Elsevier, Amsterdam, pp 309-360.

Schwarz, M. P. 1999. Definition of the Moody Suite, southern Gawler Craton. *MESA Journal*, 13, pp. 39-44.

Schwarz, M. P. 2003. *LINCOLN Map Sheet, SI 53-11*, Geological Atlas 1:250 000 Series - Explanatory Notes, South Australia, Primary Industries and Resources South Australia.

Stewart, J. R., 2010. Integrated structural geology and geophysical analysis of crustal-scale shear zones in the Gawler Craton, South Australia. PhD Thesis, Monash University, Melbourne.

Stewart, K., 1992. High temperature felsic volcanism and the role of mantle magmas in Proterozoic crustal growth : the Gawler Range volcanic province. PhD Thesis, University of Adelaide, Adelaide.

Stewart, K. & Foden, J., 2003, *Mesoproterozoic granites of South Australia*. Report book 2003/15, Primary Industries and Resources South Australia, Adelaide.

Stolz, A. J., Jochum, K. P., Spettel, B. & Hofmann, A. W. 1996. Fluid- and melt-related enrichment in the subarc mantle: evidence from Nb/Ta variations in the island-arc basalts. *Geology*, 24, pp. 587–590.

Swain, G. M., Barovich, K., Hand, M., Ferris, G. & Schwarz, M. 2008. Petrogenesis of the St Peter Suite, southern Australia: Arc magmatism and Proterozoic crustal growth iof the Southern Australian Craton. *Precambrian Research*, 166, pp. 283-296.

Swain, G. M., Woodhouse, A., Hand, M., Barovich, K., Schwarz, M. & Fanning, C. M. 2005. Provenance and tectonic development of the late Archaean Gawler Craton, Australia; U-Pb zircon, geochemical and Sm-Nd isotopic implications. *Precambrian Research*, 141, pp. 106-136.

Symington, N. J., Weinberg, R. F., Hasalová, P., Wolfram, L. C., Raveggi, M. & Armstrong, R. A. 2014. Multiple intrusions and remelting-remobilization events in a magmatic arc: The St Peter Suite, South Australia. *GSA Bulletin*, 126, pp. 1200-1218.

Szpunar, M. & Fraser, G., 2010, *Age of deposition and provenance of Palaeoproterozoic basins on north-eastern Eyre Peninsula: constraints from SHRIMP U-Pb geochronology*. Report book 2010/00008, Department of Primary Industries and Resources, South Australia, Adelaide.

Szpunar, M., Hand, M., Barovich, K. & Jagodzinski, E. J. 2011. Isotopic and geochemical constraints on the Palaeoproterozoic Hutchison Group, southern Australia: Implications for Palaeoproterozoic reconstructions. *Precambrian Research*, 187, pp. 99-126.

Teale, G. S., Schwarz, M. P. & Fanning, C. M. 2000. Potential for Archaean VHMS-style mineralisation. *MESA Journal*, 18, pp. 17-21.

Teasdale, J., 1997. The interpretive geology and tectonothermal evolution of the western Gawler Craton. PhD Thesis, Department of Geology and Geophysics, University of Adelaide,

Thomson, B. P. c., 1980. Geological map of South Australia, *Geological Atlas of South Australia, 1:1 000 000 series*. Geological Survey of South Australia.

Turner, S., Foden, J., Sandiford, M. & Bruce, D. 1993. Sm-Nd isotopic evidence for the provenance of sediments from the Adelaide fold belt and southeastern Australia with implications for episodic crustal addition. *Geochimica et Cosmochimica Acta*, 57, pp. 1837-1856.

Vassallo, J. J. & Wilson, C. J. L. 2002. Palaeoproterozoic regional-scale non-coaxial deformation: an example from eastern Eyre Peninsula, South Australia. *Journal of Structural Geology*, 24, pp. 1-24.

Wade, C. E., 2012, *Geochemistry of pre-1570 Ma mafic magmatism within Southern Australia: implications for possible tectonic settings and timing of major mineralisation events in South Australia*. Report book Report book 2012/019, Dept. for Manufacturing, Innovation, Trade, Resources and Energy., Adelaide.

Wade, C. E. & McAvaney, S. O., 2016, *Geochemistry of the Peter Pan Supersuite*. Report book 2016/00026, Department of State Development, South Australia, Adelaide.

Wade, C. E., McAvaney, S. O. & Reid, A. J., 2016. Palaeoproterozoic syn-tectonic magmatism on Eyre Peninsula: insights from new geochemistry and geochronology of the Peter Pan Supersuite*, Australian Earth Science Convention*, Adelaide, oral presentation.

Webb, A. W., Thomson, B. P., Blissett, A. H., Daly, S., Flint, R. B. & Parker, A. J. 1982. *Geochronology of the Gawler Craton, South Australia*, South Australia. Department of Primary Industries and Resources. Report Book 82/86,

Webb, A. W., Thomson, B. P., Blissett, A. H., Daly, S. J., Flint, R. B. & Parker, A. J. 1986. Geochronology of the Gawler Craton, South Australia. *Australian Journal of Earth Sciences*, 33, pp. 119-143.

Whalen, J. B., Currie, K. L. & Chappell, B. W. 1987. A-type granites: geochemical characteristics, discrimination and petrogenesis. *Contributions to Mineralogy and Petrology*, 95, pp. 407-419.

APPENDIX 1. STRATIGRAPHIC DEFINITIONS

Minbrie Gneiss (change to previous usage)

Previous usage
The first usage of the term Minbrie Gneiss was on the WHYALLA 1:250 000 Map Sheet (Parker & Flint, 1983), and was described in detail in the accompanying explanatory notes (Parker & Fanning, 1998), but was never formally defined. In these references the Minbrie Gneiss is placed within the Palaeoproterozoic (c. 1850–1690 Ma) Lincoln Complex.

Derivation of name
The derivation of the term Minbrie Gneiss was presumably taken from the Minbrie Range, where the Minbrie Gneiss is exposed, Minbrie Homestead (675756 m E 6288696 m N AGD66), Minbrie Spring (676304 m E 6289712 m N AGD66), Minbrie Springs (676226 m E 6289482 m N AGD66) or Minbrie Hill (675858 m E 6292071 m N AGD66).

Distribution
The Minbrie Gneiss is exposed in the Minbrie Range, to the east of the Cleve Hills, on eastern Eyre Peninsula. It occurs as a northeast- to north-trending curvilinear belt ~95 km long, extending from Kiaora in the south to 15 km north of Secret Rocks (previously named Refuge Rocks) in the north. This belt is ~3 km wide at its southern end, widening to ~25 km in the north.

Parent unit
The Minbrie Gneiss is herein removed from the Palaeoproterozoic Lincoln Complex, now a disused term, and placed within the Sleaford Complex (2560–2410 Ma).

Type locality
Parker & Flint (1983) and Parker & Fanning (1998) never defined a type locality for the Minbrie Gneiss, but Parker & Fanning (1998) suggest reference localities at Elbow Hill, Minbrie Springs, Salt Creek and Refuge Rocks. Descriptions of the geology of these locations can be found in Parker *et al.* (1988), Parker (1993), Fraser & Neumann (2010) and Jagodzinski & McAvaney (2016).

Lithology
The Minbrie Gneiss is a composite stratigraphic unit that contains a range of lithologies, including granitic gneiss, augen gneiss and quartz-feldspar-biotite migmatite granitic gneiss, as well as lesser sills of amphibolite and pegmatite (Parker *et al.*, 1981). Granitic gneiss comprises equigranular, medium-grained quartz-feldspar-biotite gneiss and is tonalitic to granodioritic in composition (Parker *et al.*, 1981). Augen gneiss is composed of potassium feldspar augen wrapped by a foliated medium-grained biotite-quartz-feldspar matrix. Migmatite is heterogeneous, and includes patch metatexite containing discontinuous leucosomes, net-structured metatexite containing leucosomes parallel to the gneissic fabric and in shear bands, and rafts of quartz-feldspar-biotite gneiss within leucosomes. The amphibolite sheets comprise green-brown hornblende and plagioclase, locally with minor orthopyroxene, and were emplaced prior to metamorphism of the Minbrie Gneiss (Parker *et al.*, 1981).

Relationships
The Minbrie Gneiss has an inferred structural contact with the c. 2820 Ma Coolanie Gneiss, is structurally interleaved with the Hutchison Group (c. 2000–1790 Ma) and intruded by the c. 1745–1700 Ma Peter Pan Supersuite (Parker & Fanning, 1998; Fraser & Neumann, 2010).

Depositional and emplacement age
The Minbrie Gneiss was interpreted by Parker (1993) to have been derived from the migmatisation of the Sleaford Complex, Miltalie Gneiss and early-formed Kimban granites during the Kimban Orogeny.

U-Pb zircon geochronology for orthogneiss within the Minbrie Gneiss has yielded magmatic protolith ages within the range 2521 Ma to 2418 Ma (Fraser & Neumann, 2010; Jagodzinski & McAvaney, 2016) demonstrating that this unit is a composite of felsic igneous rocks with similar mineralogy spanning the entirety of the recognized age range of the Sleaford Complex. It contains igneous units intruded at the same time as the sedimentary protoliths of the Wangary Gneiss and Carnot Gneiss were deposited and the Hall Bay Volcanics were emplaced, as well as younger igneous units intruded synchronous with the Sleafordian Orogeny (e.g. the Dutton Suite). No samples of the Sleaford Complex have yet yielded Palaeoproterozoic ages to provide evidence of protoliths equivalent to the Hutchison Group or Kimban granites (Peter Pan Supersuite).

Deformation
The deformational fabrics in the Minbrie Gneiss are generally considered to have formed during the Kimban Orogeny, when the Minbrie Gneiss underwent high temperature metamorphism and migmatisation (Parker, 1993). Zircon growth is recorded in the Minbrie Gneiss at Elbow Hill at 1733 ± 7 Ma (Fraser & Neumann, 2010). A poorly constrained age of zircon growth is also recorded in the Minbrie Gneiss at Elbow Hill at 1762 ± 43 Ma and at Elbow Hill, which may indicate that the Minbrie Gneiss underwent high grade metamorphism prior to the 1740–1690 Ma Kimban Orogeny.

Carpa Granite (change to previous usage)

Previous usage
The first usage of the term Carpa Granite was by Rutland *et al.* (1981). The term was then used on the WHYALLA 1:250 000 Map Sheet (Parker & Flint, 1983), and was described in detail in the accompanying explanatory notes (Parker & Fanning, 1998), but was never formally defined. In these references the Carpa Granite is placed within the Palaeoproterozoic (c. 1850–1690 Ma) Lincoln Complex.

Derivation of name
The derivation of the term Carpa Granite was presumably taken from Carpa Homestead (656245 m E 6263081 m N AGD66) or Carpa Waterhole (656935 m E 6262570 m N AGD66).

Distribution
Carpa Granite occurs as scattered outcrops in the Cleve Hills west of Cowell.

Parent unit
The Carpa Granite is herein removed from the Palaeoproterozoic Lincoln Complex, now a disused therm, and placed within the Sleaford Complex (2560–2410 Ma).

Type locality
The type locality of the Carpa Granite is here defined as the exposures extending around Carpa Homestead (656245 m E 6263081 m N AGD66) and Sunny-Brae Homestead (656778 m E 6262041 m N AGD66). In this area an equigranular foliated quartz-feldspar-biotite granite is exposed as whalebacks on the hill slopes.

Lithology
The Carpa Granite is massive, cream-pink, medium-grained, quartz-K-feldspar-plagioclase-biotite-muscovite granite to monzogranite with scattered aggregates of garnet (Parker *et al.*, 1981).

Relationships
The Carpa Granite is in contact with the Coolanie Gneiss, Minbrie Gneiss and Hutchison Group. Parker and Fanning (1998) describe the Carpa Granite intruding the Middle Camp Granite, although published 1:250 000 and 1:50 000 mapping shows the contact between the two granites to be fault-bound (Parker, 1978; Parker & Flint, 1983).

Depositional and emplacement age
The Carpa Granite was originally correlated with granites of the Moody Suite (c. 1700 Ma; Schwarz, 1999) on southern Eyre Peninsula due to its weak to sporadically developed fabric (Parker *et al.*, 1985), supported by a whole rock Rb-Sr age of 1677 ± 125 Ma obtained by Webb *et al.* (1986). Using a thermal ionisation mass spectrometry (TIMS) technique, Fanning (1987) obtained a multigrain U-Pb zircon age of 1994 ± 27 Ma for the Carpa Granite. This was interpreted to reflect inherited zircon within a younger granite. However, sensitive high resolution ion microprobe (SHRIMP) zircon U-Pb dating from a sample of the Carpa Granite shows that the rock was emplaced at 2517± 7 Ma and contains minor c. 3400 Ma inheritance (Fraser & Neumann, 2010). Notably, the SHRIMP analyses suggest some minor non-recent Pb loss, but do not record any evidence for zircon crystallisation during the Kimban Orogeny.

Deformation
The Carpa Granite contains a sporadically developed foliation formed during the Kimban Orogeny (Parker, 1993), ranging from undeformed through to weakly and strongly foliated.